Received: 16 May 2022 | Revised: 13 September 2022 | Accepted: 30 September 2022

DOI: 10.1111/gcb.16493

RESEARCH ARTICLE

Global Change Biology WILEY

Non-linear loss of suitable wine regions over Europe in response to increasing global warming

Giovanni Sgubin[1] | Didier Swingedouw[1] | Juliette Mignot[2] | Gregory Alan Gambetta[3] | Benjamin Bois[4] | Harilaos Loukos[5] | Thomas Noël[5] | Philippe Pieri[3] | Iñaki García de Cortázar-Atauri[6] | Nathalie Ollat[3] | Cornelis van Leeuwen[3]

[1]Environnements et Paléoenvironnements Océaniques et Continentaux (EPOC)—Université de Bordeaux, Pessac, France

[2]LOCEAN Laboratory, Institut Pierre Simon, Sorbonne Universités (SU/CNRS/IRD/MNHN), Paris, France

[3]EGFV, Bordeaux Sciences Agro, INRAE, ISVV, Univ. Bordeaux, Villenave d'Ornon, France

[4]Centre de Recherches de Climatologie, UMR 6282 CNRS/UB Biogéosciences, Univ. Bourgogne-Franche-Comté, Dijon, France

[5]The Climate Data Factory (TCDF), Paris, France

[6]INRAE, US AgroClim, Avignon, France

Correspondence
Giovanni Sgubin, Environnements et Paléoenvironnements Océaniques et Continentaux (EPOC)—Université de Bordeaux, Pessac, France.
Email: giovanni.sgubin@u-bordeaux.fr

Funding information
European Union's Horizon 2020 EUCP, Grant/Award Number: 776613

Abstract

Evaluating the potential climatic suitability for premium wine production is crucial for adaptation planning in Europe. While new wine regions may emerge out of the traditional boundaries, most of the present-day renowned winemaking regions may be threatened by climate change. Here, we analyse the future evolution of the geography of wine production over Europe, through the definition of a novel climatic suitability indicator, which is calculated over the projected grapevine phenological phases to account for their possible contractions under global warming. Our approach consists in coupling six different de-biased downscaled climate projections under two different scenarios of global warming with four phenological models for different grapevine varieties. The resulting suitability indicator is based on fuzzy logic and is calculated over three main components measuring (i) the timing of the fruit physiological maturity, (ii) the risk of water stress and (iii) the risk of pests and diseases. The results demonstrate that the level of global warming largely determines the distribution of future wine regions. For a global temperature increase limited to 2°C above the pre-industrial level, the suitable areas over the traditional regions are reduced by about 4%/°C rise, while for higher levels of global warming, the rate of this loss increases up to 17%/°C. This is compensated by a gradual emergence of new wine regions out of the traditional boundaries. Moreover, we show that reallocating better-suited grapevine varieties to warmer conditions may be a viable adaptation measure to cope with the projected suitability loss over the traditional regions. However, the effectiveness of this strategy appears to decrease as the level of global warming increases. Overall, these findings suggest the existence of a safe limit below 2°C of global warming for the European winemaking sector, while adaptation might become far more challenging beyond this threshold.

KEYWORDS
adaptation to climate change, climate change, general circulation model, phenological model, *Vitis vinifera* L.

1 | INTRODUCTION

Climate conditions are the main constraints in determining whether a specific crop is suitable to a given region and represent a crucial factor in defining the agricultural vocation of a specific area, its traditions and its economic opportunities. This is especially true for the winemaking sector, for which climate conditions establish the degree of appropriateness of a specific grapevine variety to a specific site and also determine the year-to-year yield, vintage quality and value (Jackson & Lombard, 1993). Optimal conditions for wine production depend on a vulnerable equilibrium between several climatic variables, for example temperature, solar radiation, precipitation, humidity, wind and evapotranspiration. Among them, temperature is arguably the most important factor, as it influences grapevine phenology by determining its development, from budbreak to fruit maturity (Jones & Alves, 2012), as well as affecting vine physiology and fruit metabolism/composition (Coombe, 1987). The timing of the growing stages and phenophases intervals are critical aspects in achieving an optimal ripening with a balanced level of sugars and acids in the berry (van Leeuwen et al., 2019) and an optimal development of the flavour components (van Leeuwen et al., 2022). For a given grapevine variety in the Northern Hemisphere, it has been shown that, for present-day conditions, full ripeness should ideally be reached between approximately September 10 and the October 10 (van Leeuwen & Seguin, 2006), when fruits can be harvested under relatively mild climate conditions, thus favouring the highest possible wine quality potential. Such a timing constraint requires the average temperature during the growing season to be bounded within a narrow range, which differs according to each grapevine variety, for example around 14–17°C for early ripening varieties and 17–20°C for late ripening varieties (Jones, 2006). Precipitation also plays an important role in determining an optimal ripening. On the one hand, a lack of rainfall can produce a severe decrease in grape productivity in the absence of irrigation (Moutinho-Pereira et al., 2004). On the other hand, excessive precipitation during spring increases the possibility of pests and diseases, such as downy mildew (Boso & Kassemeyer, 2008; Carbonneau, 2003) and, in general, have a detrimental effect on wine quality (van Leeuwen et al., 2009). For this reason, the most renowned quality wines are produced in regions where annual rainfall is between 500 and 800 mm/year (Anderson & Nelgen, 2020; Jackson & Schuster, 1987).

The ensemble of these climatic constraints defines a set of bioclimatic indices that have been commonly used to identify potentially suitable vineyard sites and a locally appropriate selection of grapevine varieties. Optimal climatic conditions for premium wine production can be found over a large part of Europe, where grapevine cultivation and winemaking have been practised historically (Jellinek, 1976). Today, viticulture is one of the continent's major cultural and economic patrimony: in 2018, Europe produced about 190 MhL (OIV, 2019) of wine, meaning almost 2/3 of the world production, that is, 292 MhL (OIV, 2019). Such high-volume and high-quality production condensed in a relatively small area is largely due to the presence of three main water bodies, that is, the Atlantic Ocean, the Mediterranean Sea and the Black Sea, which mitigates the climate over most of the continent and promoted the viticultural history and traditions over the centuries (Jellinek, 1976). The overall mild climate over Europe, along with large variations in soils and microclimates due to rivers, mountains, hills, or flat lands produces a considerable diversity in terms of wine typicity (Lacombe et al., 2011). It has been estimated that in Europe there are more than 1000 different typical grapevine varieties that are vinified and commercialized (Robinson et al., 2013), giving way to a policy aimed at preserving their geographic specificity (*terroir*, the base of the demarcated appellations of origin).

However, climate change might alter the existing climatic profile of these winegrowing regions, potentially affecting the boundaries of varietal suitability (Schultz & Jones, 2010). Observations over the last decades have already demonstrated that the general increase in temperature over Europe has caused an advancement of wine grape phenology (Andreoli et al., 2019; Duchêne & Schneider, 2005; García de Cortázar-Atauri et al., 2017; Ramos et al., 2008; Tomasi et al., 2011), determining alterations of the fruit composition and quality (Drappier et al., 2019; Jones & Davis, 2000; Teslic, Zinziani, et al., 2018; van Leeuwen & Darriet, 2016). Recent warming also led to significant changes of most of the bioclimatic indices over the period 1950–2009 (Santos et al., 2021).

According to the IPCC (2021), global mean surface temperature will continue to increase until at least the mid-century under all emissions scenarios considered, and the levels of global warming of 1.5 and 2°C above the pre-industrial will be exceeded during the 21st century unless deep reductions in greenhouse gas emissions occur in the coming decades. This gave rise to concern about the future viticulture over the traditional wine regions, promoting numerous studies on the zoning of future wine production in a context of global warming. At the global scale, Hannah et al. (2013) analysed an ensemble of climate projections for different emission scenarios, prefiguring a 25%–73% loss of suitable area over the major present-day wine regions by 2050 for the most pessimistic RCP8.5 emission scenario, while the loss for the RCP4.5 was just slightly lower, that is, from 19% to 62%. However, van Leeuwen et al. (2013) argued that such an assessment may overestimate potential losses, as the methodology relied on monthly mean projections and did not take into account varietal specificity in each region, nor the capacity of adaptation to warmer conditions. More recently, Morales-Castilla et al. (2020) used a set of bioclimatic indices calculated after the simulation of the onset of ripening (i.e. veraison) for 11 different varieties according to different realizations of one ocean–atmosphere general circulation model (GCM). They found that variety diversity can substantially reduce the projected losses of current winegrowing areas under warmer conditions.

At the continental scale, by defining a set of bioclimatic indices calculated using daily outputs from climate IPCC SRES projections (Meehl et al., 2007), Malheiro et al. (2010), Fraga et al. (2013) and Moriondo et al. (2013) reported a gradual northward and upward shift of climatic suitability for grapevine cultivation in Europe. Such a response implies a progressive detrimental impact on wine production over most of Southern Europe due to increasing temperature and dryness. In contrast, more suitable conditions appear in northern and central Europe, although warmer conditions over relatively wet regions may increase the risk of pests and diseases (Bois et al., 2017). By coupling CMIP5 (Taylor et al., 2012) climate projections under RCP scenarios (Meinshausen et al., 2011) with the STICS crop model (Brisson et al., 1998), Fraga et al. (2016) evidenced an enhanced dryness over the wine regions of southern Europe implying a reduction of yield and leaf area, although an overall increase of potential areas for grapevine cultivation, notably in northern Europe. The same pattern was confirmed by Cardell et al. (2019), who re-calculated the bioclimatic indices after bias-adjustment of the downscaled climate projections to more properly project climate model outputs at the local scale.

At a more regional scale, the projected increase in minimum temperatures during ripening has been shown to decrease the wine quality in the Iberian Peninsula (Fraga et al., 2012; Malheiro et al., 2012), while possible water deficit may seriously compromise future yields in Spain (Fraga et al., 2012; Malheiro et al., 2012; Yang et al., 2022). Teslic, Vujadinović, et al. (2018) showed that, by the end of the 21st century, the Emilia-Romagna region (Italy) may become completely unsuitable for winegrape production under the RCP 8.5 scenario, while its preservation may be still possible under RCP4.5, yet highly conditional on the adaptation measures to climate change that will be adopted. Koufos et al. (2017) hypothesized that warmer and drier conditions expected over Greece may possibly advance the maturity of grapevine beyond its suitability threshold, having detrimental impacts on wine quality. In contrast, climate changes are expected to be beneficial for many areas of central and northern Europe, where new vineyards may emerge (Jones & Schultz, 2016). Eitzinger et al. (2009) prefigured a doubling of potentially suitable areas for grapevine in Austria by the 2050s, in line with the expansion of wine regions predicted by Gaal et al. (2012) in Hungary, by Maciejczak and Mikiciuk (2019) in Poland and the trend evidenced in Romania (Irimia et al., 2018). New suitable areas are also expected in the UK and Wales (Nesbitt et al., 2018) as well as in Scotland (Dunn et al., 2017) and Scandinavia. A more extensive review on the impacts of climate change on European viticulture has been reported in Droulia and Charalampopoulos (2021).

Beyond these qualitative estimations of the future changes of the geography of wine regions, to date, a comprehensive quantitative assessment of the extension of both new emerging regions and of the area loss over traditional wine regions is missing at the European scale. To achieve this, we defined here a new bioclimatic index for wine production suitability, which is based on fuzzy logic and takes simultaneously into account (i) the optimal timing for fruit physiological maturity, (ii) the risk of water stress and (iii) the risk of pests and diseases. We then used this new bioclimatic index to determine the future climatic suitability for wine production across Europe, including a comprehensive assessment of uncertainty due to both climate and phenological models.

2 | METHODOLOGY

The methodology for the assessment of the climatic suitability for optimal wine production in Europe is based on five main points:

1. Coarse-resolution simulations of future climate by means of 3 CMIP5 GCMs under the RCP4.5 and RCP8.5 scenarios.
2. Dynamical downscaling of the GCM simulations over Europe with CLMcom and RCA4-SMHI regional models.
3. Bias adjustment of the model variables based on a quantile mapping method.
4. Offline coupling of the climate outputs with four phenological models for the main developmental stages of the grapevine.
5. Definition of climatic suitability indicator S for premium wine production based on the simulated phenological stages of the grapevine.

2.1 | Climate projections

We used climate projections from three different GCMs, participating to the CMIP5 project (Taylor et al., 2012), namely the CNRM-CM5 model (Voldoire et al., 2013), the EC-EARTH model (Sterl et al., 2011) and the MPI-ESM-LR model (Giorgetta et al., 2013). These models were selected as they provide gridded daily climatic data at global scale and at spatial resolution in the order of hundreds km, that is O(100 km), for the historical period (1850–2005) and future projections (2006–2100). In the historical simulations, the external boundary conditions consist of prescribed observed radiative forcing representing all known aerosols and greenhouse gases concentrations in the atmosphere estimated from observational data as well as modulations of the solar irradiance and the effect of past volcanic eruptions. Initial conditions are obtained from the O(1000)-year control (pre-industrial) simulation under fixed external forcing. Here we use historical simulation outputs from 1980 to 2005. The future projections are initialized in 2006 from the historical simulations and are forced by a common pattern of external forcing until 2100 describing different possible emission scenarios, that is the RCP scenarios (Meinshausen et al., 2011; Moss et al., 2010). Here, we analyse results from the RCP4.5 and RCP8.5 scenarios, respectively prefiguring a stabilization of radiative earth budget imbalance at 4.5 and 8.5 $W m^{-2}$ by the end of the century. The climatic variables used for our analysis are mean temperature, minimum temperature, maximum temperature and precipitation.

2.2 | Dynamical downscaling: The regional models

In order to have climate projections with a more accurate resolution of localized extreme events, we used dynamically downscaled climate projections carried out within the European CORDEX project (Jacob et al., 2014). In this framework, the outputs from the GCMs have been used to drive different regional circulation models (RCM) operating on different sub-regions and at different spatial resolution. Here we used the dynamical downscaling according with two RCMs, that is CCLM4-8-17 (CLMcom, 2016) and SMHI (Samuelsson et al., 2011), over the EUR-11 domain, which consists of a grid spacing of 0.11° (12.5 km), over the region delimited by 60.21°N, 315.86°E (top left); 66.65°N 64.4°E (top right); 22.20°N, 350.01°E (lower left); and 25.36°N, 36.30°E (lower right). A more detailed description of the downscaling method can be found on the CORDEX Internet site (http://cordex.org).

2.3 | Bias-adjustment procedure

The direct use of raw model outputs may produce partially incorrect or even unrealistic assessments, due to systematic biases affecting climate simulations. This may be notably relevant for the present study, where climate models' results are used to force different phenological models relying on cumulative thermal forcing, for which a small bias in daily temperature projections may produce a large error in the actual calculation of the pheno-phases. [Correction added on 22-Dec-2022, after first online publication: In the previous sentence, "pheno-periods" was changed to "pheno-phases".] In order to address such a potential limitation, we used bias adjusted data provided by "the Climate Data Factory" (https://theclimatedatafactory.com/). The bias-adjustment procedure relies on the Cumulative Distribution Function transform (CDF-t) method (Famien et al., 2018; Michelangeli et al., 2009; Vrac et al., 2016), which is based on the quantile mapping (QM) method (Vrac et al., 2012). It consists in the adjustment of the raw simulated temperature through a transfer function, such that its cumulative distribution function (CDF) matches the observed one over a calibration period. Here, the transfer function was calculated from EURO4M MESAN data (Bärring et al., 2014), interpolated over the EUR-11 CORDEX grid. Note that the CDF-t method also accounts for the evolution of the large-scale CDF from historical to future time period (Michelangeli et al., 2009; Vrac et al., 2012), thus preserving the long-term trends in climate models data. This characteristic makes the CDF-t method particularly suited for climate projections, and thus extensively used for impact analyses of future climate change (e.g. Vautard et al., 2013; Vrac et al., 2012; Vrac & Friederichs, 2015).

2.4 | Phenological models

The gridded daily downscaled and adjusted climatic data have been finally used to simulate the duration of the relevant phenological phases, that is, budburst, flowering, veraison and maturity, from 1980 to 2100 for different grapevine varieties. Their simulation classically relies on thermal models based on the cumulative heat (or chilling) requirement (Bonhomme, 2000). According to this approach, the day of occurrence of a given phenological phase t_p coincides with the fulfilment of a critical temperature forcing F^* formalized as of the sum of daily forcing units F_u after a certain starting day t_0:

$$t_p\colon \sum_{t_o}^{t_p} F_u = F^*. \quad (1)$$

Depending on the different assumptions for t_0 and on the different formulations for the function F_u, different types of phenological models have been developed. Here, we use four different versions, namely (i) a linear sequential model, (ii) a non-linear sequential model, (iii) a linear non-sequential model and (iv) a non-linear non-sequential model (Table 1). The different formulations of t_0 in Equation (1) identifies two main model categories: the sequential models ((i) and (ii)), in which each phenological stage after the winter dormancy is calculated starting from a previous stage (the starting day t_0 in Equation 1 is recursively calculated), and the non-sequential models ((iii) and (iv)), in which each phenological stage is calculated from a fixed day of the year (the starting day t_0 in Equation 1 is set *a priori*). These two model categories have been further discerned in two typologies, that is linear ((i) and (iii)) and non-linear models ((ii) and (iv)), depending on the definition of F_u in Equation (1). Thus, a total of four phenological models have been used, covering all the range of the state-of-the-art model typologies available in the literature. The linear models mainly rely on a linear relation between temperature and plant growing, that is the growing degree day (GDD model), based on which different targeted models have been developed (Table 1), that is, the BRIN model (Garcia de Cortazar-Atauri et al., 2009), the GFV model (Parker et al., 2013) and the GSR model (Parker et al., 2020). The non-linear models follow different formulations based either on a sigmoidal relation between temperature and plant growing, that is, the UNIFORC and UNICHILL models (Chuine, 2000), or on a curvilinear function of the WE model (Wang & Engel, 1998). Our approach is based on a clustering methodology, meaning that we apply the phenological models to different grapevine varieties. Initially, we calculated the occurrence of budburst, flowering, veraison and maturity for three grapevine varieties, which are respectively representative of three clusters of grapevine varieties depending on their different heat requirements for ripening (Parker et al., 2013, 2020; van Leeuwen et al., 2008). Chardonnay is taken as the representative for early-to-mid range ripening varieties, Syrah and Merlot for middle ripening varieties and Cabernet-Sauvignon for mid-to-late ripening varieties. The choice of these grapevine varieties has been constrained by the available published calibration and validation for the four different phenological models. Then, in order to better cover all the range of possible grapevine varieties, we also included two additional grapevine varieties clusters, namely early ripening varieties, and late ripening varieties. Their definition is based on the phenological simulations of respectively Chardonnay and Cabernet-Sauvignon, imposing that (i) the maturity day of the early ripening cluster occurs 10 days earlier than the simulated maturity day for Chardonnay, and (ii) the maturity day of the late ripening occurs 10 days later than the simulated maturity day of Cabernet-Sauvignon. We assume that grapevine maturity is generally achieved when the fruit sugar concentration is 200 g/L (Parker et al., 2020). A summary of the mean features of the four phenological model typologies is illustrated in Table 1, while their detailed formulation and calibration are respectively given in Supplementary Text 1 and Supplementary Table 1.

TABLE 1 List of adopted phenological models and their relevant bibliographic references (see Supplementary Text 1 and Supplementary Table 1 for their comprehensive formulation and calibration). GDD stands for growing degree day, which is the common formulation of the linear models. Among them, GFV stands for grapevine flowering, while GSR stands for grapevine sugar ripeness. For the non-linear models, WE stands for Wang and Engel model (Wang & Engel, 1998), whose formulation is based on a curvilinear response to temperature

	Budburst		Flowering		Veraison		Maturity	
	Model	Calibration	Model	Calibration	Model	Calibration	Model	Calibration
Linear/non-sequential	GDD	García de Cortázar-Atauri et al. (2009)	GFV	Parker et al. (2013)	GFV	Parker et al. (2013)	GSR	Parker et al. (2020)
Linear/sequential	BRIN	García de Cortázar-Atauri et al. (2009)	GDD	García de Cortázar-Atauri (2006); Valdés-Gómez et al. (2009)	GDD	García de Cortázar-Atauri (2006); Valdés-Gómez et al. (2009)	GDD	Parker (2013)
Nonlinear/non-sequential	UNIFORC	Leolini et al. (2020); Fila (2012)	Sigmoid	Fila (2012)	Sigmoid	Fila (2012)	Sigmoid	Parker et al. (2020)
Nonlinear/sequential	UNICHILL	Leolini et al. (2020); Fila (2012)	WE	García de Cortázar-Atauri et al. (2010)	WE	García de Cortázar-Atauri et al. (2010)	WE	García de Cortázar-Atauri et al. (2010)

2.5 | Suitability index

Climatic suitability for premium wine production is here defined by conditions under which the winemaking is environmentally and economically sustainable. This implies that the fruits reach their maturity under certain external conditions that can fully favour the wine quality potential, that is when grape berry technological ripeness (Carbonneau et al., 1998), phenolic ripeness (Kennedy et al., 2006) and aromatic ripeness (Noble et al., 1984; van Leeuwen et al., 2022) are reached in short time frame (van Leeuwen & Seguin, 2006). Quality and typicity are among the main sources of consumer's willingness to pay, resulting in added value in wine production (Tempere et al., 2019), thus compensating the production and vineyard management costs. Moreover, the concept of climatic suitability also implies that human activity during the grapevine growing is limited as much as possible, in order to minimize costly procedures and approaches that might affect the environmental health, such as irrigation or massive use of pesticides. Under these premises, we defined an indicator S at each grid point and for each year from 1980 to 2099, that translates the concept of climatic suitability just introduced into a measurable metric. The definition of S follows some previous studies (Fraga et al., 2013; Malheiro et al., 2010, 2012; Santos et al., 2012), in which the optimal suitability for grapevine growth was defined by the fulfilment of specific conditions on three different bioclimatic indexes, that is (1) Huglin heliothermal index (HI; Huglin, 1978), which relies on a degree-day accumulation between April and September to individuate the appropriate mean temperature conditions for grapevine growing; (2) dryness index (DI; Riou et al., 1994; Tonietto & Carbonneau, 2004), which relies on the cumulative precipitation between April and September to assess the level of dryness relevant for wine production; and (3) the hydrothermic index (HyI; Branas, 1974), which relies on both precipitation and temperature sum between April and August to estimate the risk of downy mildew disease (Carbonneau, 2003). The resulting composite index was based on Boolean logic, and its value is 1 if the conditions on the three bioclimatic indexes are simultaneously satisfied and 0 otherwise.

Our approach is also based on the definition of the climatic suitability S as a composite index accounting for temperature, precipitation and their mutual effects, but with two substantial differences compared to previous studies on changes in vineyard suitability under climate change. First, the S indicator calculated here is over the simulated phenological stages and not over a fixed period of year. This allows us to account for the potential shifts of the developmental stages of the grapevine under a warming scenario. Second, our indicator S is based on fuzzy logic, so that it can range between 0 and 1. This allows us to handle the concept of "partial" suitability, as S may capture all the range of degree of suitability between fully optimal conditions ($S = 1$) and completely unsuitable conditions ($S = 0$). Under these premises, we define the composite climatic suitability indicator S as:

$$S = S_M S_P S_z, \tag{2}$$

where S_M, S_P and S_Z are dimensionless indexes between 0 and 1.

The S_M index indicates whether the simulated day of maturity falls within the temporal windows for an optimal fruit development. Its definition is conceptually similar to the HI index, that is, the first component of the composite index in Malheiro et al. (2010), Santos et al. (2012), Malheiro et al. (2012), Fraga et al. (2013), as it primarily depends on the heat accumulation requirement of the grapevine. Following the formulation made in Hannah et al. (2013), we assume here that the climatic conditions for S_M are fully suitable if the mean temperature of the 30 days preceding the maturity occurrence is bounded between 22°C (T_{OPT1} in Figure 1a) and 15°C (T_{OPT2} in Figure 1a), while it linearly decreases for the 25 days beyond these temperature limits (Figure 1a). The temporal window for full suitability has been, in any case, constrained between two limit days of the year (DOY), that is, the 10 August and the 10 November. This means that maturity reached before the 15 July or after the 5 December yields to a null suitability S_M. We also tested two different formulations of the optimal window for maturity, under two alternative definitions of T_{OPT1} and T_{OPT2}, that is respectively (i) by using the minimum temperature in place of mean temperature and (ii) by using fixed days of the year (see Supplementary Text 2 for more details).

The S_P index indicates whether the soil–water availability due to precipitation is enough to prevent excessive water deficit during the plant growth. The imposed conditions are based on the conditions used in Malheiro et al. (2010), Santos et al. (2012), Malheiro et al. (2012), Fraga et al. (2013) for the DI, but calculated over the period between budburst and veraison, in a simplified manner, as follows:

$$\mathrm{DI} = W_0 + \sum_{t=\mathrm{BUD}}^{t=\mathrm{VER}} (P - k \times \mathrm{ET}_0), \tag{3}$$

where W_0 is the initial soil water reserve at field capacity (mm), here assumed to be constant for each year at the budburst day, that is, $W_0 = 200$ mm; P is the simulated daily precipitation (mm); k is a non-dimensional crop coefficient; which here is considered constant, that is, $k = 0.5$; and ET_0 is the reference evapotranspiration (mm) calculated, for each grid point, from the simulated air temperature according with the Hargreaves formula (Hargreaves & Samani, 1985), under the assumption of constant initial useful soil-water reserve. This formulation implies that vineyard evapotranspiration is a constant fraction of ET_0 throughout the grapevine growing season, thus not accounting for the increase in grapevine transpiration as leaf area grows and for the changes in grapevine stomatal regulation under limited water availability. According to Fraga et al. (2013), the S_P index is 0 if the DI index is lower than −100 mm (severe water deficit), and it linearly increases for values between −100 and 100 mm, beyond which the hydric conditions are considered as optimal, that is, $S_P = 1$ (Figure 1b). It is worth noticing that the conditions in Figure 1b have been applied for the DI calculated at the veraison day and not at the maturity day to account for the fact that a moderate water deficit during grape ripening is beneficial for the wine quality (van Leeuwen et al., 2009).

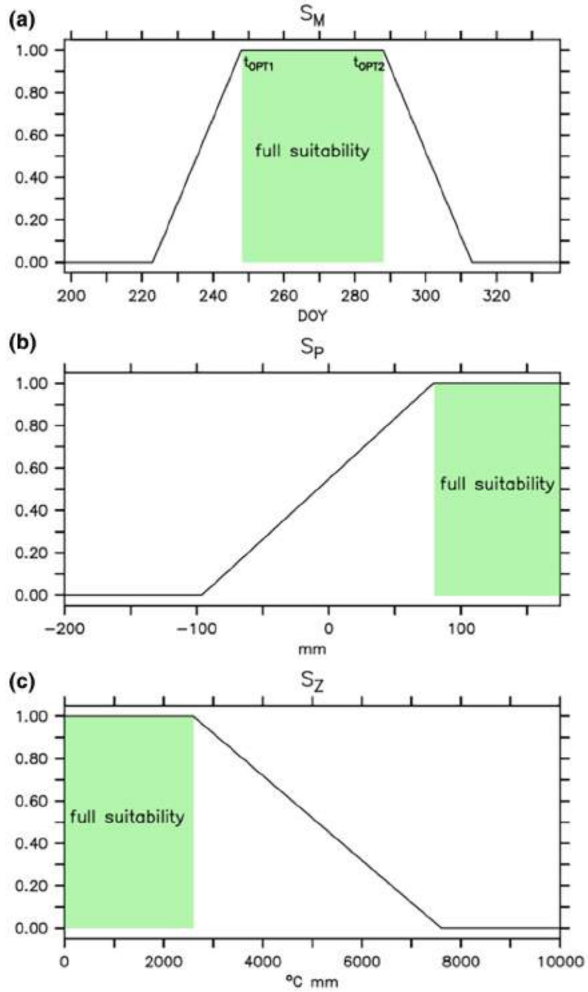

FIGURE 1 Schematic of the methodology used for (a) the calculation of S_M; (b) the calculation of S_P; and (c) the calculation of S_Z. Following their definitions given in Section 2, the three indexes are plotted against (a) the day of maturity, (b) the dryness index (DI) (Equation 3) and (c) the hydrothermic index (Equation 4). The green regions indicate the conditions of full suitability, which are bounded by specific limits. For S_M, these limits coincide with the first day for which the following 30-days mean temperature is below 22°C (T_{OPT1}) and the first day for which the following 30-days mean temperature is below 15°C (T_{OPT2}). For S_P and S_Z the limits are based on those defined in Fraga et al. (2013).

Finally, the S_Z index indicates whether the combination of conditions on temperature and precipitation are suitable to prevent the risk of severe plant diseases. The imposed conditions are based on those used in Malheiro et al. (2010), Santos et al. (2012), Malheiro et al. (2012), Fraga et al. (2013) for the HyI index (Figure 1c), but calculated over the period between budburst and maturity:

$$\mathrm{HyI} = c \times \sum_{t=\mathrm{BUD}}^{t=\mathrm{MAT}} (P \times T), \tag{4}$$

where P is the simulated daily precipitation (mm) and T is the simulated daily temperature (°C), and $c = (\mathrm{DOY}_{MAT} - \mathrm{DOY}_{BUD}) / 152$ is a scaling factor to comply with the threshold values in Malheiro et al. (2010), Santos et al. (2012), Malheiro et al. (2012), Fraga et al. (2013), that is the number of days between the simulated budburst and maturity divided by the number of days between the 1 April and the 30 August, that is, 152 days. Following the definition of suitability in Malheiro et al. (2010), Santos et al. (2012), Malheiro et al. (2012), Fraga et al. (2013), the S_Z index is 0 for HyI > 7500°C mm, while we set the full suitability, that is, $S_Z = 1$, for HyI < 2600°C mm (Figure 1c).

2.6 | Extension of suitable regions for wine production

To quantify the extension of suitable regions for high quality wine production, we first calculate the best S score (Equation 2) among the five grapevine clusters for each grid point. This metric estimates the maximum potential for a given region to produce high quality wine, independently of the precocity of the chosen grapevine variety, thus identifying an additional cluster, hereafter simply referred to as *Vitis vinifera*. Moreover, we introduce a threshold L for the indicator S and, for a given period, we define a region as climatically suitable for wine production when this threshold is exceeded. We tested sensitivity of the suitable areas to the threshold L in the range from 0.50 to 0.75, and chose the value that best represented the present-day distribution of suitable areas over Europe (Johnson & Robinson, 2013), that is, $L = 0.65$.

To define a reference pattern against which the future evolution of climatic suitability for wine production can be assessed, we calculate the mean *V. vinifera* suitability index S over a 30-year baseline period, that is, 1980–2009, and we identify the surface mask for which it exceeds the threshold L. We target the resulting surface mask as the traditional wine region, and we consider it as the present-day suitable region. We then analyse the evolution of suitable areas from this reference pattern by identifying the surface mask for which the condition $S > L$ is satisfied for *V. vinifera* in climate projections. Finally, we assess, for a specific period after 2009, the extension of (i) new wine regions and (ii) area loss over the traditional wine regions over a specific period of the future. We define the former as the measure of suitable areas outside the mask of the traditional wine region, while the latter is the portion inside the mask of the traditional wine region that does not satisfy the condition $S > L$ anymore.

2.7 | Varietal diversity and potential benefits of varietal turnover in future climate

The suitability for *V. Vinifera* over a specific region implies that this region is climatically suitable for at least one of the five grapevine varieties considered here. Nevertheless, a given region may be climatically suitable for more than one of these varieties, thus introducing the concept of varietal diversity, that we define here as the number of different grapevine varieties that simultaneously satisfy the suitability conditions $S > L$. The varietal diversity represents an additional factor to be considered when assessing the evolution of the geography of wine, as in many traditional wines actually different varieties are being used. Also, the varietal diversity indicates, to some extent, the potential adaptivity of a given region, as it measures the range of possible variety turnover allowed according to the characteristic local climatic conditions.

To quantify the benefits coming from a varietal turnover as a possible adaptation measure to climate change, the assessment of area loss over traditional wine regions presented above for *V. vinifera* has been finally extended to the single grapevine variety. We hypothesize two different approaches: (i) a conservative approach, in which a specific variety is supposed to be fixed over the time and (ii) a flexible approach, in which we consider the possibility to replace one specific variety with a more climatically suitable one. By using the definition of climatic suitability given above, that is, $S > L$, we estimate the area loss within the traditional regions for these two approaches, and we evaluate their differences. This eventually allows for an assessment of the portion of suitable area within the traditional regions that can be potentially preserved to wine production when adopting a flexible approach.

2.8 | Uncertainty attribution to cause

All the outcomes here are based on a set of different model simulations, which implies an uncertainty of their ensemble mean. Since each simulation relies on a specific GCM g, downscaled with a specific RCM r, and coupled with a specific phenological model p, there are three main sources of uncertainty. In this regard, following a similar approach as in Hawkins and Sutton (2009) and Lehner et al. (2020), we quantify the uncertainty of the results related to each of these components. For a given emission scenario, the prediction S_v of a specific variable v at time t, can be assumed to be partitioned as:

$$S_v(t,g,r,p) \approx \overline{S_v}(t) + \Delta_{GCM}(t,g) + \Delta_{RCM}(t,r) + \Delta_{PHENO}(t,p), \quad (5)$$

where $\overline{S_v}(t)$ is ensemble mean of all the 24 simulations at time $t = 1, 2, ..., 120$, Δ_{GCM} is the deviation due to GCM g (with $g = 1, 2, 3$), Δ_{RCM} is the deviation due to the RCM r (with $r = 1, 2$), and Δ_{PHENO} is the deviation due to the phenological model p (with $p = 1, 2, 3, 4$). This formulation allows us to isolate three different sources of uncertainty, that is, the one associated with (i) different GCMs, (ii) different RCMs and (iii) different phenological models. Indeed, from Equation (5), the total uncertainty σ_{tot} of the 24 simulations can be approximated to a summation of variances σ^*_{tot} as follows:

$$\sigma_{tot}(t) \approx \sigma^*_{tot}(t) = \sigma_{GCM}(t) + \sigma_{RCM}(t) + \sigma_{PHENO}(t), \quad (6)$$

where σ_{GCM} is the variance of the means of the eight simulations performed with the three GCMs, σ_{RCM} is the variance of the means of the 12 simulations performed with the two RCMs and σ_{RCM} is the variance of the means of the six simulations performed with the four phenological models. Therefore, the fractional uncertainty from a given source is respectively calculated as $\sigma_{GCM}(t)/\sigma^*_{tot}(t)$; $\sigma_{RCM}(t)/\sigma^*_{tot}(t)$; and $\sigma_{PHENO}(t)/\sigma^*_{tot}(t)$. This formulation assumes that the three sources of uncertainty are additive, which presupposes that the three terms $\Delta_{GCM}, \Delta_{RCM}, \Delta_{PHENO}$ in Equation (5) are orthogonal. This is an acceptable assumption in this specific context, since GCMs, RCMs and phenological models are formally independent. We performed the analysis on the uncertainty on two variables of interest: (i) the total suitable area over Europe and (ii) the percentage of area loss over the traditional regions, which will be the core variables of our results.

3 | RESULTS

3.1 | Present-day distribution of suitable areas for high quality wine

The starting point of this analysis focuses on the qualitative evolution of the pattern of the simulated suitable areas for high quality wine production from the baseline period (Figure 2) to the future (Figures 3 and 4). The definition of suitable area (see Section 2) is a function of the absolute suitability index S for each variety, whose pattern from 1980 to 2100 (Figure S1) is determined by the different contributions of S_M (Figure S2), S_P and S_Z (Figure S3), as described in Supplementary Text 3. In the upper panel of Figure 2, the contoured regions delimit the potential suitable area for *V. vinifera* for $L = 0.65$ (see Section 2) over the baseline period, that is what we refer to as traditional wine regions here-in-after. Within this area, each location has been characterized by its best suited grapevine variety, identified according with the maximum S indicator among the five grapevine clusters (Figure S1). Most of the simulated wine regions are located between the southernmost part of Europe and 48°N (as also sketched in Figure S1), covering more than 90% of the total suitable area. Earlier grapevine varieties meet best climatic conditions mainly north of 45°N and in the hilly and sub-mountain regions of southern Europe, while later grapevine varieties are best suited in the coastal regions of the Atlantic and Mediterranean sectors south of 45°N. The Figure 2b shows the map of varietal diversity for the baseline period. High potential for grapevine diversity covers most of the regions between 40°N and 46°N. In this latitude band, some regions like Bordeaux (France), La Rioja (Spain), Douro (Portugal) and Tuscany (Italy) appear currently as the most adaptive, since, on average, suitable climatic conditions subsist for all the five grapevine clusters here analysed. Along with these regions showing a high potential for varietal diversity, also regions showing a low varietal diversity determined by high S scores for earlier grapevine varieties, for example Loire, Burgundy and Alsace (France), Baden (Germany), Trentino (Italy), have to be considered as potentially adaptive regions in a context of global warming. In contrast, most critical regions are those characterized by high S scores for only later grapevine varieties, for example Alentejo (Portugal), Extremadura and Catalonia (Spain), Po Valley, Apulia and Sicily (Italy), and in general most of the coastal regions of the Mediterranean. The overall pattern significantly overlaps with the actual growing areas for

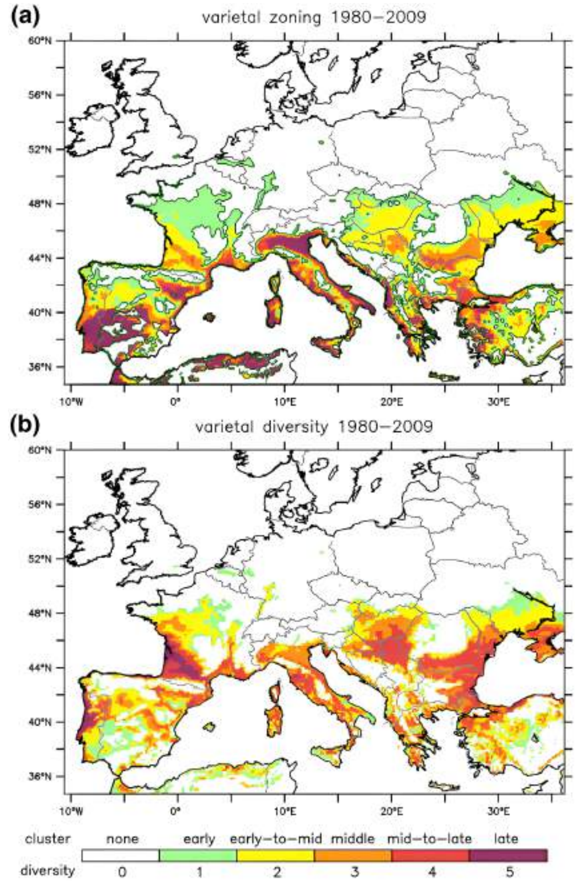

FIGURE 2 Pattern of (a) the best suited grapevine variety and (b) the varietal diversity for the baseline period 1980–2009. The *dark green contours* in the upper panel identify the simulated suitable region for wine production over the baseline period, that is, the traditional region of wine production. *Black contours* mark the coastal outlines, including major estuaries. *Light grey contours* indicate the country's borders, included here for better geo-referencing the suitability features. Map lines delineate study areas and do not necessarily depict accepted national boundaries.

present-day conditions yielding confidence in our modelling approach. Sensitivity tests performed with different values of L have been presented in the Supplementary Information. The use of both less restrictive thresholds L, for example $L = 0.50$, and more restrictive thresholds, for example $L = 0.75$, for the definition of suitable areas brings qualitatively similar results (Figure S4). A similar pattern has been also found when using the two alternative methods for the definition of S_M as illustrated in Figure S5.

3.2 | Change of the spatial distribution of suitable areas due to climate change

Under future warming conditions, results show an alteration of the geography of wine production (Figures 3 and 4), reflecting the anomaly pattern evidenced in Figure S6 for the suitability index S. The latter is, in turn, determined by the projected anomalies of the indicators S_M (Figure S7), S_P (Figure S8), and S_Z (Figure S9),

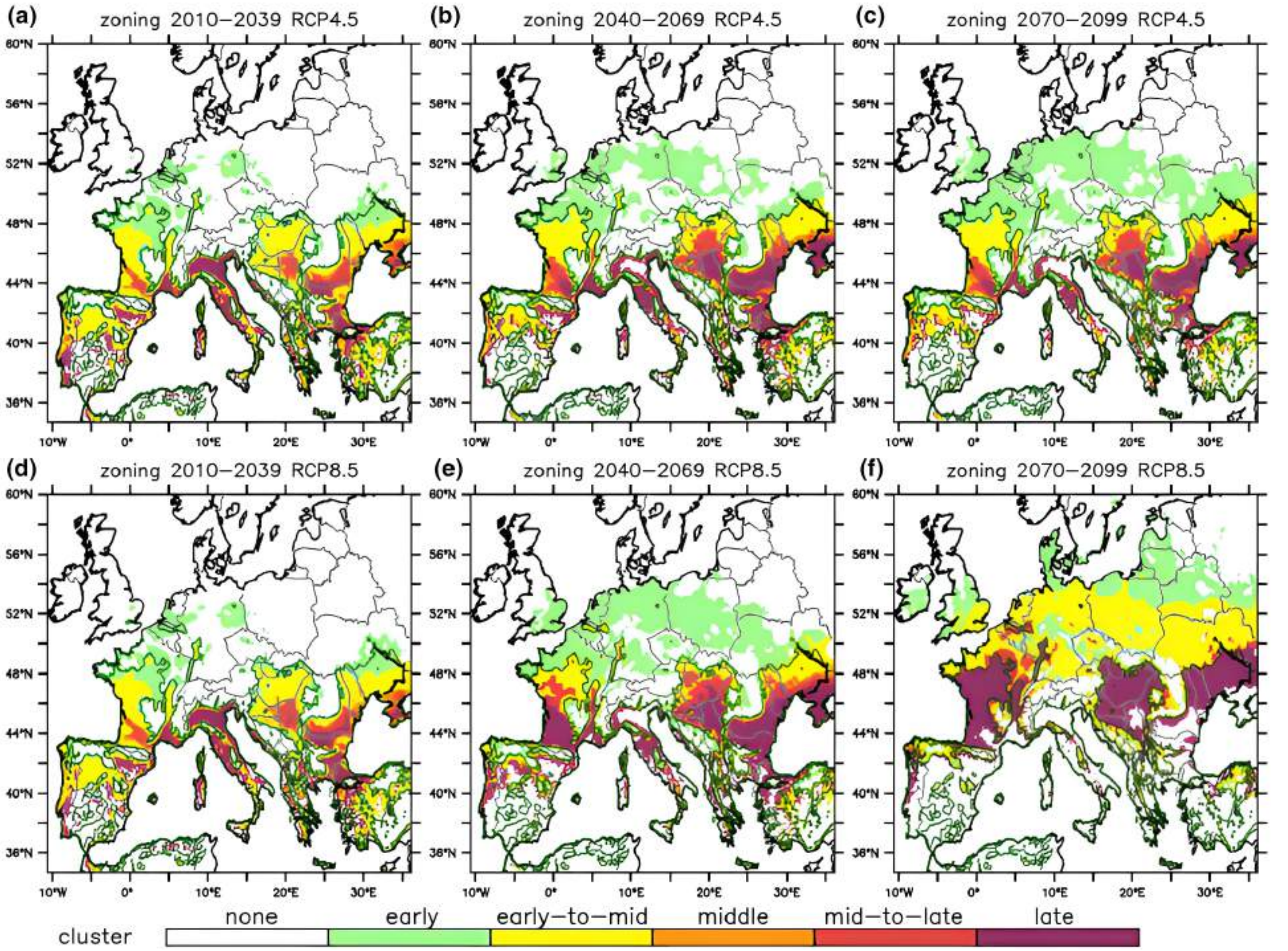

FIGURE 3 Mean pattern of the best suited grapevine variety for: (left panels, i.e. (a) and (d)) the period 2010–2039; (middle panels, i.e. (b) and (e)) the period 2040–2069; (right panels, i.e. (c) and (f)) the period 2070–2099. Upper panels, i.e. (a), (b) and (c), are relative to climate projections under RCP4.5 scenario, while lower panels, i.e. (d), (e) and (f), are relative to climate projections under RCP8.5 scenario. *Dark green contours* identify the simulated suitable region for wine production over the baseline period. *Black contours* mark the coastal outlines, including major estuaries. *Light grey contours* indicate the country's borders, included here for better geo-referencing the suitability features. Map lines delineate study areas and do not necessarily depict accepted national boundaries.

as described in Supplementary Text 4. For both emission scenarios, the identified wine regions shift northward, while southern Europe is characterized by a gradual reduction of suitable areas, which is strongly dependent on the level of global warming. For RCP4.5, this loss appears mainly limited to flat regions south of about 40°N (upper panels of Figure 3). [Correction added on 22-Dec-2022, after first online publication: In the previous sentence, "figure 5" was changed to "figure 3".] Most of the southern part of Spain appears to become unsuitable for wine production already in the period 2010–2039 (Figure 3a), while climatic conditions start to be gradually unsuitable in southern Portugal, Sicily, Apulia and Po Valley (Italy) in the subsequent periods analysed (Figure 3b,c). Over the rest of the traditional wine regions the climatic suitability is maintained, as well as the main zoning (Figure 3) and diversity features (Figure 4). At the end of the century, 90% of the of the suitable areas are located south of 52°N, although new wine regions extend up to 56°N, thus interesting the southern part of the U.K., the northern part of Germany and a substantial part of Poland and Ukraine. For the RCP8.5 scenario (lower panels of Figure 3), both losses over traditional wine regions and new suitable areas are more extended, notably for the projections of the second part of the 21st century. For the period 2010–2039 (Figure 3d), the zoning pattern is still very similar to the one in RCP4.5 (Figure 3a), while suitable area loss becomes increasingly consistent starting from the period 2040–2069 (Figure 3e). At the end of the century, results show that more than 90% of the suitable areas are located between 44°N and 56°N, thus evidencing a mean northward shift of about 8° with respect to the baseline period. In this scenario, most of the traditional wine growing regions over Portugal, Spain, Italy and Greece identified in Figure 2 become climatically unsuitable for high quality production, while over the south of France and Hungary viticulture only remains sustainable with the adoption of later-ripening varieties (Figure 3f). In contrast, the latitude band between 48°N and 52°N shows the best potential for wine diversification, notably in the Atlantic sector, where climatic conditions become optimal for all the five different grapevine varieties here analysed (Figure 4f).

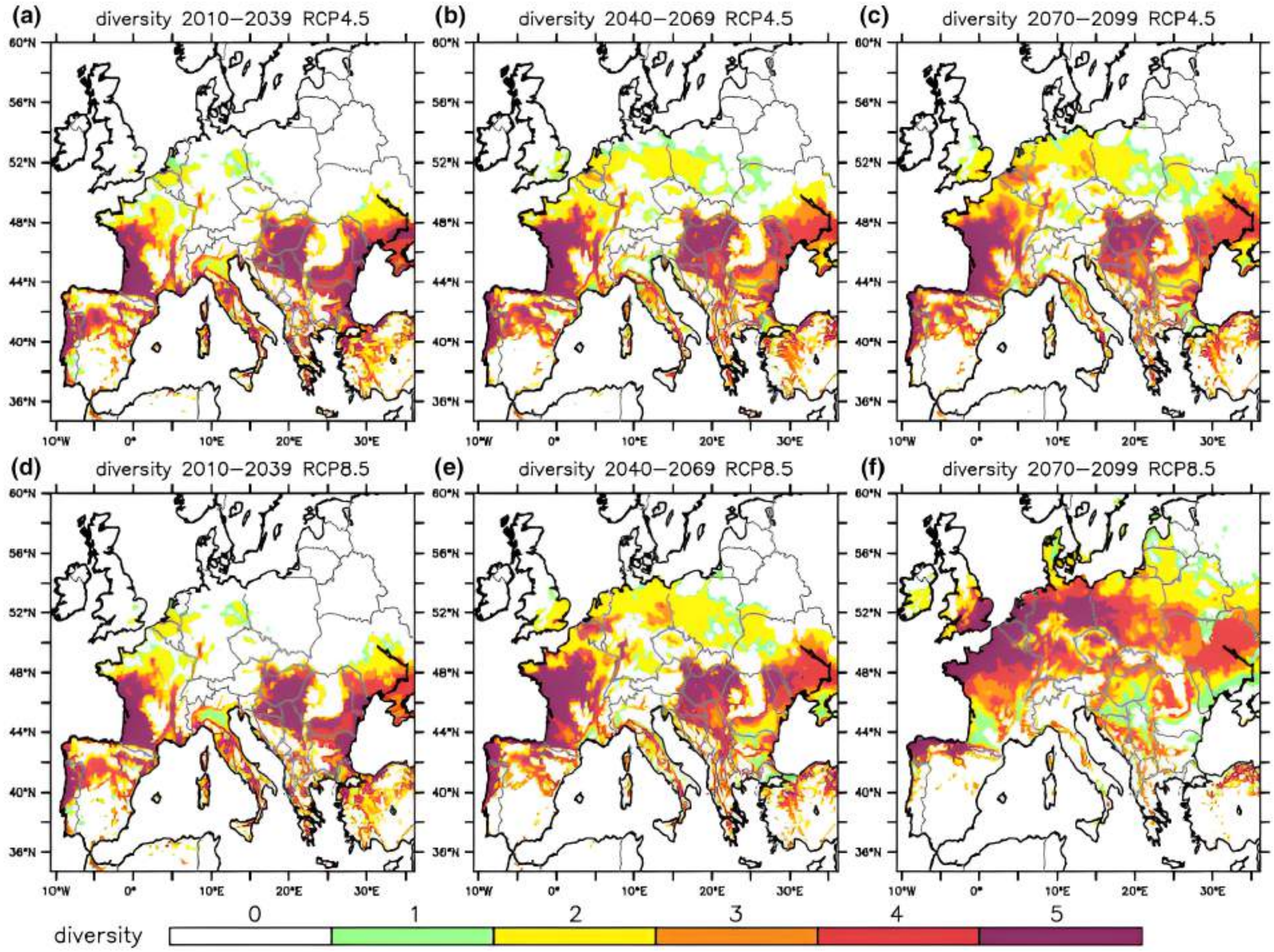

FIGURE 4 Mean pattern of the grapevine varietal diversity for: (left panels, i.e. (a) and (d)) the period 2010–2039; (middle panels, i.e. (b) and (e)) the period 2040–2069; (right panels, i.e. (c) and (f)) the period 2070–2099. Upper panels, i.e. (a), (b) and (c), are relative to climate projections under RCP4.5 scenario, while lower panels, i.e. (d), (e) and (f), are relative to climate projections under RCP8.5 scenario. *Black contours* mark the coastal outlines, including major estuaries. *Light grey contours* indicate the country's borders, included here for better geo-referencing the suitability features. Map lines delineate study areas and do not necessarily depict accepted national boundaries.

3.3 | Quantifying the area loss over the traditional regions

To quantify the extension of new emerging wine regions and to estimate the area loss over traditional wine regions, we calculate the evolution of the suitable areas outside and inside the contoured region in Figure 2a. The suitable surface in traditional regions is approximately the same for RCP4.5 and RCP8.5 scenarios until around 2040, when the area loss is estimated to be 10% with respect to the recent-past configuration (Figure 5a). The extension of new emerging regions is also similar until around 2040 (Figure 5b), when they represent around 35% of the total suitable area over Europe. In general, the expansion of new wine regions compensates for the area loss over traditional regions, thus making the overall suitable regions across Europe more extended when compared to the recent-past (Figure 5c). This trend is maintained also after 2040. At the end of the century, depending on the emission scenario, the total suitable regions for wine production are 33% to 45% greater than in the recent past (Figure 5c). However, both scenarios show a significant difference regarding the way in which this enlargement of potential wine regions is reached after 2040. For RCP4.5 scenario, the area loss over traditional regions is less than 20% at the end of the century (Figure 5a), when the overall potentially suitable regions (Figure 5c) appear equally distributed between traditional (Figure 5a), and new wine regions (Figure 5b). On the contrary, for the RCP8.5, after 2040, both the rise of new potential wine regions and the loss in traditional regions are more pronounced, thus producing larger winegrowing region shifts with respect to those for RCP4.5. At the end of the century, emerging suitable regions have a surface area that is three times greater than traditional wine regions, thus overturning much more clearly the geography of wine production with respect to the recent past configuration. [Correction added on 22-Dec-2022, after first online publication: In the previous sentence, “are three times more extended” was changed to “have a surface area that is three times greater”.] The growing gap between the results with RCP4.5 and RCP8.5 scenarios suggests a non-linear evolution of wine region extension under different levels of global warming.

In Figure 6, we focus on the relative loss of suitable area over the identified traditional wine regions in function of the simulated increase

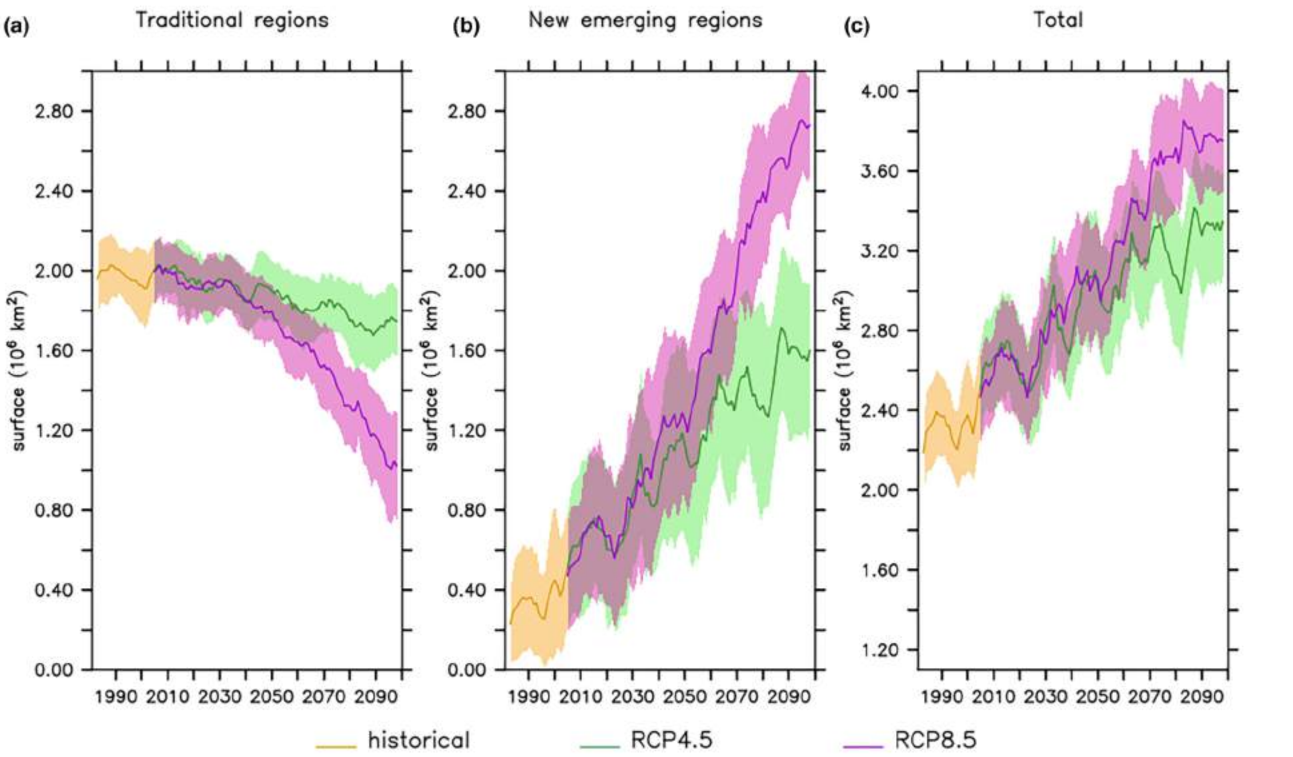

FIGURE 5 Evolution of the absolute suitable area for wine production, that is, *Vitis vinifera* cluster, (a) within the traditional boundaries for wine production, that is, over the traditional wine regions identified over the baseline period; (b) outside the traditional boundaries for wine production; (c) over the whole of Europe.

of global temperature. In particular, results for all the 24 realizations have been displayed for RCP8.5 scenario, which covers, depending on the GCM considered, a range of global warming with respect to pre-industrial conditions from roughly 0.5 to 4.5°C. The plot clearly evidences that the rate of relative area loss increases for increasing levels of global warming, independently of the model realization. For global temperature anomalies below 2°C, the mean relative area loss is estimated to be 3.9%/°C, while for higher values of global warming this loss trend is estimated to be 17.1%/°C. As far as the RCP8.5 scenario is concerned, this means, for example, that the area loss due to an additional warming of 1°C in 2070 (for which the level of global warming is already above the 2°C) is more than four times larger than the area loss due to a warming of 1°C in 2020. Such a feature is not dependent on the methodology used, as the same behaviour has been found for both alternative values of the threshold *L* previously defined and for the alternative methods used for the definition of S_M (Figure S10). This clearly highlights the strong nonlinearity of the response of traditional viticulture regions to global warming, with large changes projected to happen beyond the threshold of 2°C of global warming.

3.4 | The source of uncertainty

Both Figures 5 and 6 evidence some uncertainties in the calculation of the absolute and relative area loss over traditional wine regions. The relative contribution to the total spread of these three components has been sketched in Figure 7. The source of uncertainty in the estimation of the extension of suitable area over traditional wine regions (Figure 5a) is notably associated with the different phenological models adopted, whose spread explains, on average, 52.5 ± 5.6% and 52.9 ± 5.9% of the total uncertainty for RCP4.5 and RCP8.5 scenarios respectively (Figure 7a,b). The different GCMs are responsible of 32.5 ± 4.5% and 33.1 ± 5.3% of the total uncertainty for RCP4.5 and RCP8.5 scenarios respectively, while the contribution of RCMs is more marginal, that is, 14.9 ± 3.9% for RCP4.5 and 14.0 ± 3.9% for RCP8.5. Nevertheless, phenological models appear generally more consistent in estimating the percentage of traditional area loss for levels of global warming below 2°C, explaining, on average, less than 20% of the total uncertainty before about 2040 for both RCP45 and RCP8.5 (Figure 7c,d). Over this period, the total uncertainty is primarily due to the different GCMs' results, that is, 59.5 ± 8.7% for RCP4.5 and 58.5 ± 5.8% for RCP8.5 scenario, while the spread associated with the different RCMs has a minor impact (Figure 7c,d). The spread between phenological models increases as the global temperature increases, and, beyond a certain level of global warming, the uncertainty due to phenological inter-model spread becomes more important than the one associated with GCMs. Under RCP8.5 scenario, at the end of the century 45.0% of the total variance is associated with the different phenological models, while the fraction attributable to the different GCMs amounts to 38.3%. It is worth noticing that, despite these uncertainty features, the main behaviours evidenced in Figure 6 do not depend on the

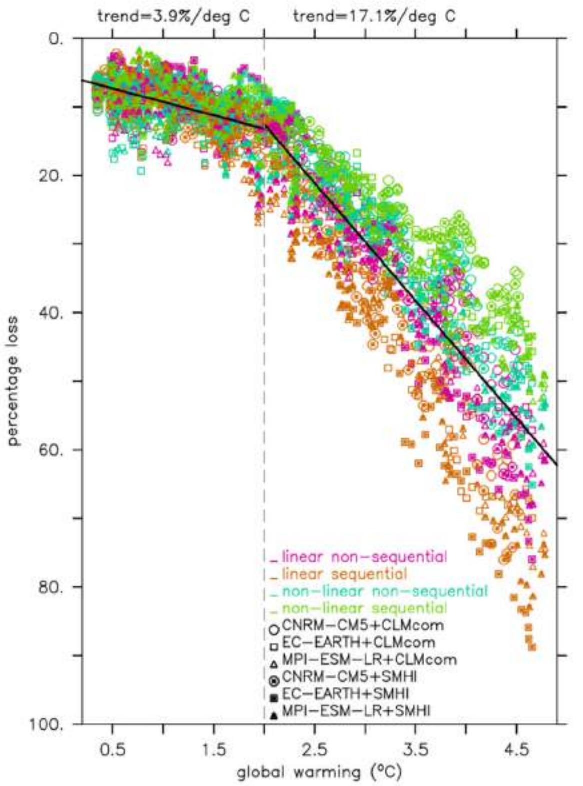

FIGURE 6 Scatterplot of the simulated relative area loss for *Vitis vinifera* cluster over the traditional wine regions (%) versus the projected global temperature anomaly (°C) with respect to the pre-industrial level. *Circles*, *squares* and *triangles* indicate the simulations performed with the CNRM-CM5, the EC-EARTH and the MPI-ESM-LR global models respectively. *Empty* and *full* symbols indicate dynamical downscaling with the CLMcom and SMHI regional models respectively. *Violet symbols* indicate the coupling with linear/non-sequential phenological model; *orange symbols* indicate the coupling with linear/sequential phenological model; *cyan symbols* indicate the coupling with non-linear/non-sequential phenological model; and *green symbols* indicate the coupling with non-linear/sequential phenological model. *Solid black lines* indicate the mean trends before and after the 2°C level of global warming. The latter has been evidenced through the *dashed grey line*.

specific model considered. Indeed, the ratio between the rate of loss for levels of warming above 2°C and below 2°C is similar for all the 24 realizations, that is, this ratio is always greater than four.

3.5 | The effectiveness of adaptation measures at different levels of global warming

Exploiting the varietal diversity at different levels of global warming found in Figure 5, may be a practicable long-term measure of adaptation to climate change (Duchêne et al., 2010; Morales-Castilla et al., 2020; Santos et al., 2021). Indeed, due to the different thermal requirements among the different grapevine varieties, it is possible to substantially reduce the detrimental effects of increasing temperatures over traditional wine regions by replacing one specific variety with a more climatically suitable one, that is, through the so-called varietal turnover. After having tested in Figure S11 the robustness of the assumption made for the total uncertainty partition (Equation 6), in Figure 8, we compare the relative loss of suitable area over traditional wine regions using two different scenarios: in the first one, no long-term adaptation measures have been allowed, while in the second one, varietal shifts to more appropriate grapevine variety have been implemented. The respective percentages of area loss have been quantified by averaging the results for the five varietal clusters over four different 20-year future periods, and for both emission scenarios. Varietal turnover appears more effective for limited values of global warming. Indeed, for each grapevine variety, the portion of suitable area loss that would be maintained through varietal turnover decreases for increasing global temperatures. As an example, for middle range ripening varieties under RCP8.5 scenario, the percentage of suitable area loss in 2020–2039 is 4.7% if varietal shift is allowed and 18.8% otherwise, while it is respectively 54.2% against 78.4% in 2080–2099. This means that for a global warming of 1.65 ± 0.12°C (that is, the mean value over the period 2020–2039), 75% of the potential area loss with no adaptation allowed would be retained thanks to varietal turnover, while for global warming of 3.85 ± 0.13°C (that is, the mean value over the period 2080–2099), variety turnover is an effective solution for only 31% of the potential area loss. This behaviour is amplified for earlier ripening clusters because of their larger potential for a varietal replacement, while it gradually eases for the later ripening clusters up to vanishing for the late ripening cluster, for which varietal shift is intrinsically precluded.

4 | DISCUSSION

Our assessments are based on the definition of a new climatic suitable indicator, which allowed us to gather a set of key features characterising the methodology of some previous studies on climatic suitability for wine production. In this framework, our approach was simultaneously based on: (i) a multi-model analysis, in order to maximize the robustness of the results and to evaluate the uncertainty associated with the models (similarly to Hannah et al., 2013); (ii) dynamically downscaled climate projections, providing relatively high spatial resolution over Europe, that is, 12.5 km, in order to capture most of the local scale climatic features (similarly to Fraga et al., 2013, where, however, the spatial resolution was 25 km); (iii) de-biased climate projections, in order to minimize the intrinsic errors associated with climate models (similarly to Cardell et al., 2019); (iv) bioclimatic indicators calculated over the simulated phenological phases and not over a fixed period of the year, in order to take into account the likely future contractions of the different grapevine growing phases (similarly to Morales-Castilla et al., 2020); (v) a subdivision of the *V. vinifera* varieties into five different variety clusters, in order to take into account the different thermal requirements of the grapevine families and the possibility of varietal turnover in the future (similarly to Morales-Castilla et al., 2020). [Correction added on 22-Dec-2022, after first online publication: In the previous sentence, "Indeed" was changed to "In this

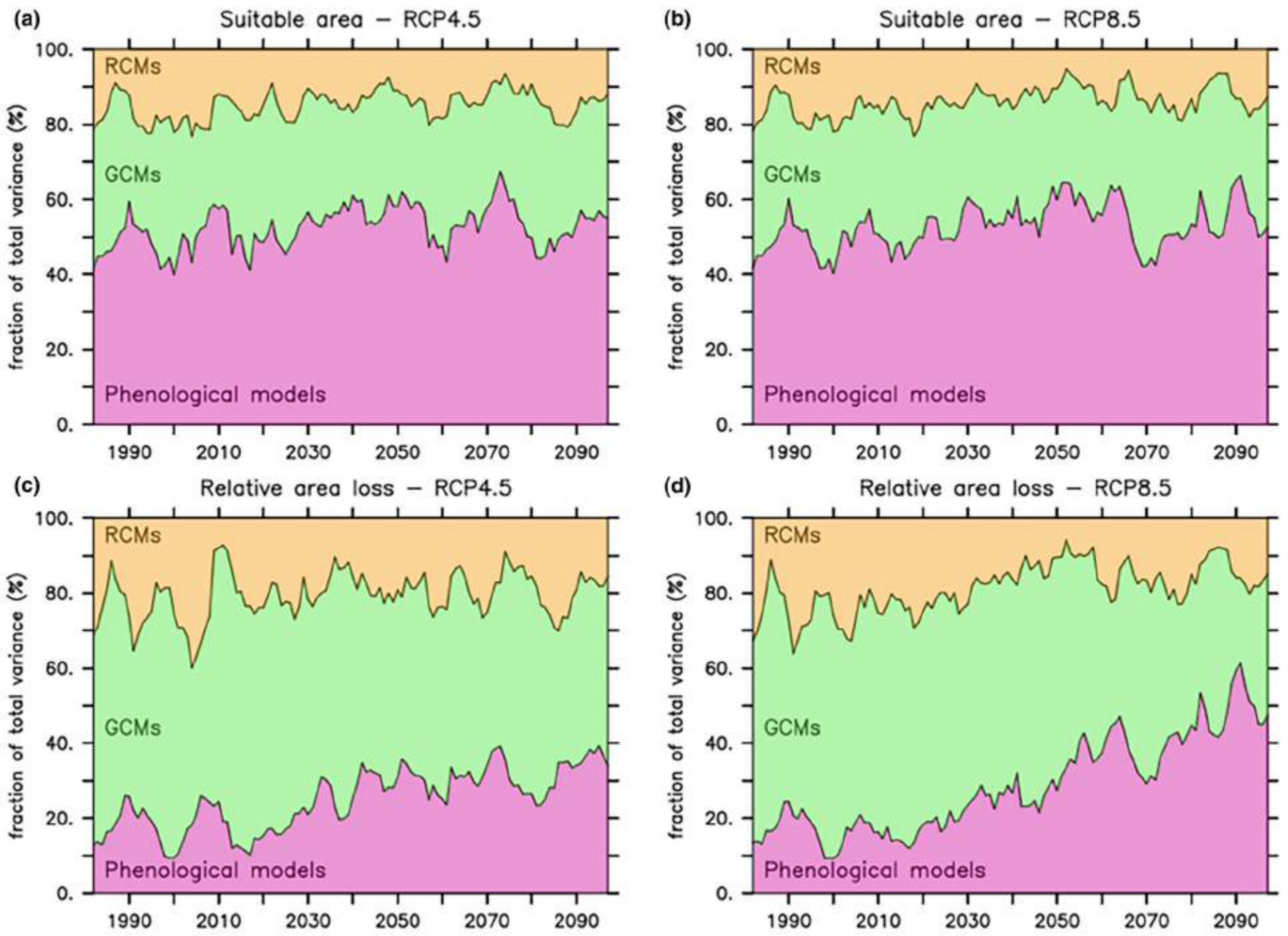

FIGURE 7 The sources of uncertainty in (upper panels, i.e. (a) and (b)) the estimation of suitable area in the traditional regions and (lower panels, i.e. (c) and (d)) the relative loss over the traditional regions, for (left panels, i.e. (a) and (c)) RCP4.5 scenario and (right panels, i.e. (b) and (d) RCP8.5 scenario. The relative uncertainty of the three main components is expressed as the fraction of the approximated total variance σ^{*}_{tot} (Equation 6). *Violet portions* represent the relative uncertainty associated with Phenological Models; *green portions* represent the relative uncertainty associated with GCMs; and *orange portions* represent the relative uncertainty associated with RCMs.

framework" .] All these features were used together to analyse the impact of climate change on viticulture in Europe. It is important to note that our estimations of traditional area loss did not significantly depend on the assumptions made in our experimental design. Both different formulations of the S_M and different values of the threshold L for the definition of suitable area (see Section 2) yielded similar relative changes in the geography of wine. [Correction added on 22-Dec-2022, after first online publication: In the previous sentence, "Indeed, both" was changed to "Both".] Overall, this study provides an overview on the future threats and opportunities for viticulture all over Europe, and might therefore promote local analyses with a finer spatial resolution than 12.5 km, allowing for capturing additional features like topographic slopes and the presence of water bodies.

One caveat of the present study can be related to the fact that the identification of suitable regions for wine production, for both the recent past and the future, was based only on climatic conditions and varietal choices. However, the actual suitability at a given location is also dependent on the specific soil features, on the level of urbanization and on the presence or absence of different crops. [Correction added on 22-Dec-2022, after first online publication: In the previous sentence, "Indeed" was changed to "However".] These factors were not considered in the present study, neither were market forces, which are critical in determining the selling price of the wines, and thus the economic sustainability of its production. Moreover, the assumption that a balanced maturity occurs for grapevine sugar concentration of 200 g/L may have led to the exclusion of some regions that are actually devoted to wine production. Indeed, optimal sugar concentration at harvest may be significantly different from 200 g/L when targeting specific wine types. For example, the production of sparkling wines like Champagne (France) or Franciacorta (Italy) requires a high acidity and a lower sugar concentration (around 170 g/L), while some dessert wines like Passito (Italy) or Sherry (Spain) require higher sugar concentrations (250–260 g/L). Nevertheless, the overall simulated boundaries of wine regions and the spatial distribution of their different varieties over Europe for the recent past (Figure 2) accurately reflects the observed geography of the winegrowing regions across the continent (Johnson & Robinson, 2013). This general agreement can be considered as

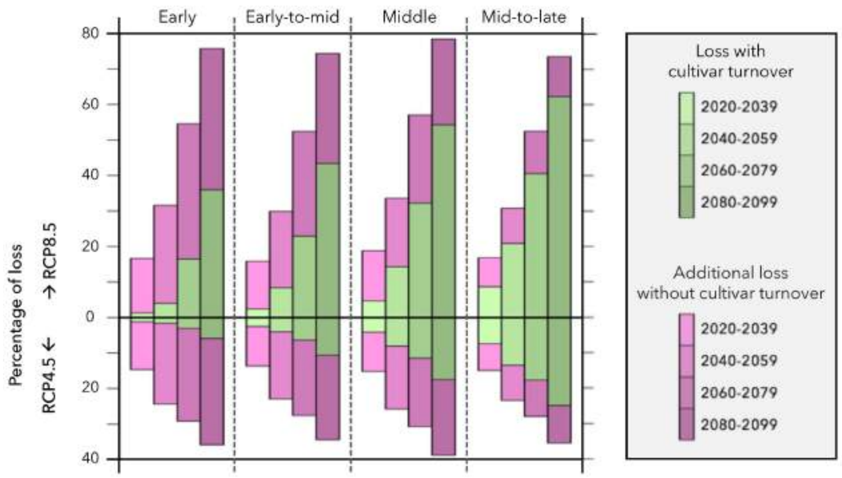

FIGURE 8 Simulated percentage of area loss over the traditional wine regions for the five grapevine clusters, for (*lower histograms*) RCP4.5 and (*upper histograms*) RCP8.5 scenario. *Green bars* are relative to estimates for which cultivar turnover (i.e. grapevine variety replacement with a more climatically suited one) is included. *Purple bars* are relative to the estimates of the additional area loss when cultivar turnover is not included. Different shades of green and purple bars indicate different periods over which these estimates have been performed. These estimates regard the early varieties (*first block*), the early-to-mid varieties (*second block*), the middle range varieties (*third block*) and the mid-to-late varieties (*fourth block*). The estimates for late varieties are not included here because the difference between a scenario with varietal turnover and a scenario without varietal turnover would be null.

a validation of our methodology, thus confirming the reliability for our assessments at the continental scale, with very few exceptions.

Future approaches following this study should include the coupling between climate models and plant/crop models allowing both for a more in depth analysis of the fruit composition and the berry size, as well as for a more sophisticated simulation of soil and plant water relations. Indeed, here, we assumed that the soil water reserve was fully recovered to a standard value every year at budburst. While generally valid, this assumption may be unrealistic in some regions with low winter rainfall, notably in the context of global warming. Moreover, our water balance modelling did not account for stomatal regulation of grapevine in response to water deficit (Lebon et al., 2003). A more accurate simulation of water availability by means of plant/crop models would therefore likely impact the calculation of the S_p index, thus possibly exacerbating or limiting the climatic suitability losses due to water stress shown here, notably for Southern Europe.

Another aspect that was not considered here was the impact of extreme meteorological events. Recent studies showed that heat waves may provoke a decrease in the yield by up to −35% in some regions (Fraga et al., 2020). Also, the occurrence of spring frosts may substantially damage the buds and reduce both yield and quality (Poling, 2008). Including these factors in our analysis would likely strengthen the nonlinear relation we found here between the increase of global temperature and the suitable area loss in traditional wine regions. The frequency of heat waves has been projected to increase in the future (Brown, 2020) as well as their intensity and length (Molina et al., 2020), thus possibly accelerating the suitability loss in traditional regions, and slowing the emergence of new wine regions. The same is true if spring frost events are also taken into account, since the risk of their occurrence has been shown to increase in some regions under warmer global conditions (Molitor et al., 2014; Mosedale et al., 2015; Sgubin et al., 2018).

The variation between the results from the different phenological models appeared to be the main source of uncertainty in our assessments. This reveals the need for testing the reliability of the different phenological models in the context of global warming, which would allow the selection of the best performing models for narrowing the uncertainty in results of suitability projections. In this context, it is worth mentioning that the uncertainty associated with GCMs may be underestimated in this study. Being constrained by the availability of simultaneously dynamically downscaled and de-biased climate projections, we used only three GCMs, whose spread in projecting future temperature represent just a fraction of the total uncertainty among the CMIP5 models. According to a CMIP5 model clustering in function of their projected temperature evolution (Sgubin et al., 2017), the three GCMs used here belong to the same cluster of models, thus not fully covering the wide range of possible temperature evolution over Europe. In particular, the chance of abrupt cooling events over the North Atlantic were not accounted for in the present study. These events, although less likely than a gradual increase of temperature throughout the 21st century (Sgubin et al., 2017; Swingedouw et al., 2021), have been shown to have possibly a strong impact on temperature over the continent and thus on the determination of suitable regions for wine production (Sgubin et al., 2019).

5 | CONCLUSION

In this study, we analysed the possible alterations of the geography of wine production in Europe under different scenarios of global warming. We explored both the emergence of new wine regions and the area loss from traditional regions through the definition of new climatic suitability index accounting for the variations in grapevine phenology of five different varietal clusters. At the end of the 21st century, results showed a northward shift of suitable regions for wine production up to 3° of latitude for the RCP4.5 scenario, and up to 8° for the RCP8.5 scenario. These shifts produced a net expansion of the total suitable areas of 33% for RCP4.5 scenario, and 45% for RCP8.5 scenario, but concurrently with an area loss of about 20% for RCP4.5 and about 55% for RCP8.5 from traditional wine regions. Therefore, the suitability loss over the traditional regions represents a major threat for the production of high-quality wine in Europe.

While a direct relation between long-term increases of temperature and detrimental effects for wine production over traditional regions was already reported in literature (e.g. Hannah et al., 2013; White et al., 2006), we showed that such a relation is not linear. In particular, we assessed that in the absence of long-term adaptation measures to global warming the loss of suitable areas over traditional wine regions is more than four times faster for levels of global warming exceeding 2°C than for global warming limited to 2°C. According to our assessment, this means that an augmentation of 1°C today would provoke a reduction of about 4% in the extension of traditional regions, while a further augmentation of 1°C would imply an additional reduction of about 17%. Moreover, we showed that grapevine varietal turnover, which is one of the viable long-term adaptation measures for wine producers to limit the effects of climate change (Morales-Castilla et al., 2020; Santos et al., 2021), is decreasingly effective for increasing levels of global warming.

These findings suggest the existence of a tolerable limit of global warming for viticulture in Europe, which might be relevant in policy discussions and definition of the best strategies to cope with climate change (Hoegh-Guldberg et al., 2018). In this regard, we quantitatively demonstrated the crucial importance of maintaining the level of global warming below 2°C above pre-industrial levels for the preservation of the traditional wine regions across Europe, thus highlighting an additional sector for which the detrimental effects of climate change are non-linear but tend to amplify beyond a certain limit. This reinforces the urgent needs invoked in the latest United Nations Climate Change Conferences to push for a more effective mitigation strategy at global scale.

ACKNOWLEDGMENTS

This work received support from the Blue-Action (European Union's Horizon 2020 research and innovation program, Grant 1668 No. 727852) and EUCP (European Union's Horizon 2020 research and innovation programme under Grant Agreement No. 776613) projects, as well as from the French government in the framework of the University of Bordeaux's IdEx “Investments for the Future” program/RRI Tackling Global Change. This study benefited from the ESPRI computing and data centre (https://mesocentre.ipsl.fr) which is supported by CNRS, Sorbonne University, Ecole Polytechnique and CNES as well as through national and international grants. Finally, the authors wish to thank three anonymous reviewers for their valuable help in improving the manuscript.

CONFLICT OF INTEREST

The authors declare no competing interests.

DATA AVAILABILITY STATEMENT

The climate data supporting the findings of this study are openly available at the following URL: https://climate4impact.eu.

ORCID

Giovanni Sgubin https://orcid.org/0000-0002-0190-0188
Didier Swingedouw https://orcid.org/0000-0002-0583-0850
Juliette Mignot https://orcid.org/0000-0002-4894-898X
Gregory Alan Gambetta https://orcid.org/0000-0002-8838-5050
Harilaos Loukos https://orcid.org/0000-0001-5417-5947
Thomas Noël https://orcid.org/0000-0003-2953-5060
Iñaki García de Cortázar-Atauri https://orcid.org/0000-0001-6941-9844
Cornelis van Leeuwen https://orcid.org/0000-0002-9428-0167

REFERENCES

Anderson, K., & Nelgen, S. (2020). *Which winegrape varieties are grown where? A global empirical picture (Revised Edition)*. University of Adelaide Press. https://www.adelaide.edu.au/press/titles/winegrapes

Andreoli, V., Cassardo, C., La Iacona, T., & Spanna, F. (2019). Description and preliminary simulations with the Italian Vineyard Integrated Numerical Model for estimating physiological values (IVINE). *Agronomy*, *9*, 94. https://doi.org/10.3390/agronomy9020094

Bärring, L., Landelius, T., Wilcke, R. A. I., Dahlgren, P., Nikulin, G., Villaume, S., Undén, P., & Kållberg, P. (2014). *A new high-resolution European region reanalysis dataset for RCM evaluation and calibration—First tests and comparison to other datasets*. RCM2014 Workshop Proceedings, 3rd International Lund RCM Workshop: 21st Century Challenges in Regional-scale Climate Modelling, Lund, Sweden, 16–19 June 2014.

Bois, B., Zito, S., & Calonnec, A. (2017). Climate vs grapevine pests and diseases worldwide: The first results of a global survey. *OENO One*, *51*(2), 133–139. https://doi.org/10.20870/oeno-one.2017.51.2.1780

Bonhomme, R. (2000). Bases and limits to using degree-day units. *European Journal of Agronomy*, *13*, 1–10. https://doi.org/10.1016/S1161-0301(00)00058-7

Boso, S., & Kassemeyer, H. H. (2008). Different susceptibility of European grapevine cultivars for downy mildew. *Vitis*, *47*(1), 39–49. https://doi.org/10.5073/vitis.2008.47.39-49

Branas, J. (1974). *Viticulture*. Imp. Dehan.

Brisson, N., Mary, B., Ripoche, D., Jeuffroy, M.-H., Ruget, F., Nicoullaud, B., Gate, P., Devienne-Barret, F., Antonioletti, R., Durr, C., Richard, G., Beaudoin, N., Recous, S., Tayot, X., Plenet, D., Cellier, P., Machet, J. M., Meynard, J. M., & Delécolle, R. (1998). STICS: A generic model for the simulation of crops and their water and nitrogen balances. I. Theory and parameterization applied to wheat and corn. *Agronomie*, *18*, 311–346. https://doi.org/10.1051/agro:19980501

Brown, S. J. (2020). Future changes in heatwave severity, duration and frequency due to climate change for the most populous cities. *Weather and Climate Extremes*, *30*, 100278. https://doi.org/10.1016/j.wace.2020.100278

Carbonneau, A. (2003). Ecophysiologie de la vigne et terroir. In *Terroir, zonazione, viticoltura. Trattato internazionale* (pp. 61–102). Phytoline.

Carbonneau, A., Champagnol, F., Deloire, A., & Sévila, F. (1998). Récolte et qualité du raisin. In C. Flanzy (Ed.), *Œnologie. Fondements scientifiques et technologiques* (pp. 647–668). Lavoisier Tec & Doc ed..

Cardell, M. F., Amengual, A., & Romero, R. (2019). Future effects of climate change on the suitability of wine grape production across Europe. *Regional Environmental Change*, *19*, 2299–2310. https://doi.org/10.1007/s10113-019-01502-x
Chuine, I. (2000). A unified model for budburst of trees. *Journal of Theoretical Biology*, *207*, 337–347. https://doi.org/10.1006/jtbi.2000.2178
CLMcom. (2016). *CLMcom CORDEX data for Europe (EUR-11) based on CCLM4-8-17 model simulations*. World Data Center for Climate (WDCC) at DKRZ. http://cera-www.dkrz.de/WDCC/ui/Compact.jsp?acronym=CXEU11CLCL
Coombe, B. G. (1987). Influence of temperature on composition and quality of grapes. *Acta Hortoculturae*, *206*, 23–36. https://doi.org/10.17660/actahortic.1987.206.1
Drappier, J., Thibon, C., Rabot, A., & Geny-Denis, L. (2019). Relationship between wine composition and temperature: Impact on Bordeaux wine typicity in the context of global warming: Review. *Critical Reviews in Food Science and Nutrition*, *59*, 14–30. https://doi.org/10.1080/10408398.2017.1355776
Droulia, F., & Charalampopoulos, I. (2021). Future climate change impacts on European viticulture: A review on recent scientific advances. *Atmosphere*, *12*, 495. https://doi.org/10.3390/atmos12040495
Duchêne, É., Huard, F., Dumas, V., Schneider, C., & Merdinoglu, D. (2010). The challenge of adapting grapevine varieties to climate change. *Climate Research*, *41*, 193–204. https://doi.org/10.3354/cr00850
Duchêne, E., & Schneider, C. (2005). Grapevine and climatic changes: A glance at the situation in Alsace. *Agronomy for Sustainable Development*, *25*, 93–99. https://doi.org/10.1051/agro:2004057
Dunn, M., Rounsevell, M. D. A., Boberg, F., Clarke, E., Christensen, J., & Madsen, M. S. (2017). The future potential for wine production in Scotland under high-end climate change. *Regional Environmental Change*, *19*, 723–732. https://doi.org/10.1007/s10113-017-1240-3
Eitzinger, J., Kubu, G., Formayer, H., & Gerersdorfer, T. (2009). *Climatic wine growing potential under future climate scenarios in Austria*. Sustainable Development and Bioclimate: Reviewed Conference Proceedings, Vienna, Austria, pp. 146–147.
Famien, A. M., Janicot, S., Ochou, A. D., Vrac, M., Defrance, D., Sultan, B., & Noel, T. (2018). A bias-corrected CMIP5 dataset for Africa using the CDF-t method—A contribution to agricultural impact studies. *Earth System Dynamics*, *9*, 313–338. https://doi.org/10.5194/esd-9-313-2018
Fila, G. (2012). *Modelli matematici per l'analisi della variabilità spazio-temporale della fenologia della vite* (Ph.D. thesis). University of Padova.
Fraga, H., García de Cortázar-Atauri, I., Malheiro, A. C., & Santos, J. A. (2016). Modelling climate change impacts on viticultural yield, phenology and stress conditions in Europe. *Global Change Biology*, *22*, 3774–3788. https://doi.org/10.1111/gcb.13382
Fraga, H., Malheiro, A. C., Moutinho-Pereira, J., & Santos, J. A. (2012). An overview of climate change impacts on European viticulture. *Food and Energy Security*, *1*, 94–110. https://doi.org/10.1002/fes3.14
Fraga, H., Malheiro, A. C., Moutinho-Pereira, J., & Santos, J. A. (2013). Future scenarios for viticultural zoning in Europe: Ensemble projections and uncertainties. *International Journal of Biometeorology*, *57*(6), 909–925. https://doi.org/10.1007/s00484-012-0617-8
Fraga, H., Molitor, D., Leolini, L., & Santos, J. (2020). What is the impact of heatwaves on European viticulture? A modelling assessment. *Applied Sciences*, *10*, 3030. https://doi.org/10.3390/app10093030
Gaal, M., Moriondo, M., & Bindi, M. (2012). Modelling the impact of climate change on the Hungarian wine regions using Random Forest. *Applied Ecology and Environmental Research*, *10*, 121–140. https://doi.org/10.15666/aeer/1002_121140
García de Cortázar-Atauri, I. (2006). *Adaptation du Modèle STICS à la Vigne (Vitis vinifera L.): Utilisation dans le cadre d'une étude d'impact du changement climatique à l'échelle de la France* (PhD. thesis). École Nationale Supérieure Agronomique.
García de Cortázar-Atauri, I., Brisson, N., & Gaudillère, J. P. (2009). Performance of several models for predicting budburst date of grapevine (*Vitis vinifera* L.). *International Journal of Biometeorology*, *53*, 317–326. https://doi.org/10.1007/s00484-009-0217-4
García de Cortázar-Atauri, I., Chuine, I., Donatelli, M., Parker, A. K., & van Leeuwen, C. (2010). *A curvilinear process-based phenological model to study impacts of climatic change on grapevine* (Vitis vinifera *L.)*. Proceedings of Europeen Society for Agronomy Congress, August 2010, Montpellier, France. https://hal.inrae.fr/hal-02824232
García de Cortázar-Atauri, I., Duchêne, E., Destrac, A., Barbeau, G., de Resseguier, L., Lacombe, T., Parker, A. K., Saurin, N., & van Leeuwen, C. (2017). Grapevine phenology in France: From past observations to future evolutions in the context of climate change. *OENO One*, *51*, 115–126. https://doi.org/10.20870/oeno-one.2017.51.2.1622
Giorgetta, M. A., Jungclaus, J., Reick, C. H., Legutke, S., Bader, J., Böttinger, M., Brovkin, V., Crueger, T., Esch, M., Fieg, K., Glushak, K., Gayler, V., Haak, H., Hollweg, H. D., Ilyina, T., Kinne, S., Kornblueh, L., Matei, D., Mauritsen, T., … Stevens, B. (2013). Climate and carbon cycle changes from 1850 to 2100 in MPI-ESM simulations for the coupled model intercomparison project phase 5. *Journal of Advances in Modeling Earth Systems*, *5*, 572–597. https://doi.org/10.1002/jame.20038
Hannah, L., Roehrdanz, P. R., Ikegami, M., Shepard, A. V., Shaw, M. R., Tabor, G., Zhi, L., Marquet, P. A., & Hijmans, R. J. (2013). Climate change, wine, and conservation. *Proceedings of the National Academy of Sciences of the United States of America*, *110*, 6907–6912. https://doi.org/10.1073/pnas.1210127110
Hargreaves, G., & Samani, Z. (1985). Reference crop evapotranspiration from temperature. *Applied Engineering in Agriculture*, *1*, 96–99. https://doi.org/10.13031/2013.26773
Hawkins, E., & Sutton, R. (2009). The potential to narrow uncertainty in Regional Climate Predictions. *Bulletin of the American Meteorological Society*, *90*, 1095–1108. https://doi.org/10.1175/2009BAMS2607.1
Hoegh-Guldberg, O., Jacob, D., Taylor, M., Bindi, M., Brown, S., Camilloni, I., Diedhiou, A., Djalante, R., Ebi, K., Engelbrecht, F., Guiot, J., Hijioka, Y., Mehrotra, S., Payne, A., Seneviratne, S. I., Thomas, A., Warren, R., & Zhou, G. (2018). Impacts of 1.5°C global warming on natural and human systems. In V. Masson-Delmotte, P. Zhai, H.-O. Pörtner, D. Roberts, J. Skea, P. R. Shukla, A. Pirani, W. Moufouma-Okia, C. Péan, R. Pidcock, S. Connors, J. B. R. Matthews, Y. Chen, X. Zhou, M. I. Gomis, E. Lonnoy, T. Maycock, M. Tignor, & T. Waterfield (Eds.), *Global warming of 1.5°C. An IPCC Special Report on the impacts of global warming of 1.5°C above pre-industrial levels and related global greenhouse gas emission pathways, in the context of strengthening the global response to the threat of climate change, sustainable development, and efforts to eradicate poverty*. IPCC.
Huglin, P. (1978). Nouveau mode d'évaluation des possibilités héliothermiques d'un milieu viticole. *Comptes Rendus de l'Académie d'Agriculture de France*, *64*, 1117–1126.
IPCC (2021). Summary for Policymakers. In V. Masson-Delmotte, P. Zhai, A. Pirani, S. L. Connors, C. Péan, S. Berger, N. Caud, Y. Chen, L. Goldfarb, M. I. Gomis, M. Huang, K. Leitzell, E. Lonnoy, J. B. R. Matthews, T. K. Maycock, T. Waterfield, O. Yelekçi, R. Yu, & B. Zhou (Eds.), *Climate change 2021: The physical science basis. Contribution of working group I to the sixth assessment report of the Intergovernmental Panel on Climate Change* (pp. 3–32). Cambridge University Press. https://doi.org/10.1017/9781009157896.001
Irimia, L. M., Patriche, C. V., & Roșca, B. (2018). Climate change impact on climate suitability for wine production in Romania. *Theorical Applied Climatolology*, *133*, 1–14. https://doi.org/10.1007/s00704-017-2156-z
Jackson, D., & Schuster, D. (1987). Production of grapes in cool climates. In *Wine grapes: A complete guide to 1368 vine varieties, including their origins and flavours*. Butterworths.
Jackson, D. I., & Lombard, P. B. (1993). Environmental and management practices affecting grape composition and wine quality—A review. *American Journal of Enology and Viticulture*, *44*(4), 409–430.

Jacob, D., Petersen, J., Eggert, B., Alias, A., Christensen, O. B., Bouwer, L. M., Braun, A., Colette, A., Déqué, M., Georgievski, G., Georgopoulou, E., Gobiet, A., Menut, L., Nikulin, G., Haensler, A., Hempelmann, N., Jones, C., Keuler, K., Kovats, S., … Yiou, P. (2014). EURO-CORDEX: New high-resolution climate change projections for European impact research. *Regional Environmental Change*, *14*, 563–578.

Jellinek, E. M. (1976). Drinkers and alcoholics in ancient Rome. *Journal of Studies on Alcohol*, *37*(11), 1718–1740.

Johnson, H., & Robinson, J. (2013). *The world atlas of wine* (7th revised & updated edition). Mitchell Beazley.

Jones, G. V. (2006). Climate and terroir: Impacts of climate variability and change on wine. In R. W. Maqueen & L. D. Meinert (Eds.), *Fine wine and terroir—The geoscience perspective*. Geoscience Canada Reprint Series Number 9. Geological Association of Canada.

Jones, G. V., & Alves, F. M. (2012). Impact of climate change on wine production: A global overview and regional assessment in the Douro Valley of Portugal. *International Journal of Global Warming*, *4*, 383. https://doi.org/10.1504/IJGW.2012.049448

Jones, G. V., & Davis, R. E. (2000). Climate influences on grapevine phenology, grape composition, and wine production and quality for Bordeaux, France. *American Journal of Enology and Viticulture*, *51*, 249–261.

Jones, G. V., & Schultz, H. R. (2016). Climate change and emerging cool climate wine regions. *Wine and Viticulture Journal*, *31*, 51–53.

Kennedy, J. A., Saucier, C., & Glories, Y. (2006). Grape and wine phenolics: History and perspective. *American Journal of Enology and Viticulture*, *57*(3), 239–248. https://www.ajevonline.org/content/57/3/239

Koufos, G., Mavromatis, T., Koundouras, S., & Jones, G. V. (2017). Response of viticulture-related climatic indices and zoning to historical and future climate conditions in Greece. *International Journal of Climatology*. https://doi.org/10.1002/joc.5320

Lacombe, T., Audeguin, L., Boselli, M., Bucchetti, B., Cabello, F., Chatelet, P., Crespan, M., D'Onofrio, C., Dias, J. E., Ercisli, S., Gardiman, M., Grando, M. S., Imazio, S., Jandurova, O., Jung, A., Kiss, E., Kozma, P., Maul, E., Maghradze, D., … This, P. (2011). Grapevine European catalogue: Towards a comprehensive list. *Vitis*, *50*, 65–68.

Lebon, E., Dumas, V., Pieri, P., & Schultz, H. R. (2003). Modelling the seasonal dynamics of the soil water balance of vineyards. *Functional Plant Biology*, *30*, 699–710. https://doi.org/10.1071/FP02222

Lehner, F., Deser, C., Maher, N., Marotzke, J., Fischer, E. M., Brunner, L., Knutti, R., & Hawkins, E. (2020). Partitioning climate projection uncertainty with multiple large ensembles and CMIP5/6. *Earth System Dynamics*, *11*, 491–508. https://doi.org/10.5194/esd-11-491-2020

Leolini, L., Costafreda-Aumedes, S., Santos, J. A., Menz, C., Fraga, H., Molitor, D., Merante, P., Junk, J., Kartschall, T., Destrac-Irvine, A., van Leeuwen, C., Malheiro, A. C., Eiras-Dias, J., Silvestre, J., Dibari, C., Bindi, M., & Moriondo, M. (2020). Phenological model intercomparison for estimating grapevine budbreak date (*Vitis vinifera* L.) in Europe. *Applied Sciences*, *10*, 3800. https://doi.org/10.3390/app10113800

Maciejczak, M., & Mikiciuk, J. (2019). Climate change impact on viticulture in Poland. *International Journal of Climate Change Strategies and Management*, *11*, 254–264. https://doi.org/10.1108/IJCCSM-02-2018-0021

Malheiro, A. C., Santos, J., Fraga, H., & Pinto, J. (2010). Climate change scenarios applied to viticultural zoning in Europe. *Climate Research*, *43*, 163–177. https://doi.org/10.3354/cr00918

Malheiro, A. C., Santos, J. A., Fraga, H., & Pinto, J. G. (2012). Future scenarios for viticultural climatic zoning in Iberia. *Acta Horticulturae*, *931*, 55–61. https://doi.org/10.17660/ActaHortic.2012.931.5

Meehl, G. A., Stocker, T. F., Collins, W. D., Friedlingstein, P., Gaye, A. T., Gregory, J. M., Kitoh, A., Knutti, R., Murphy, J. M., Noda, A., Raper, S. C. B., Watterson, I. G., Weaver, A. J., & Zhao, Z.-C. (2007). Global climate projections. In S. Solomon, D. Qin, M. Manning, Z. Chen, M. Marquis, K. B. Averyt, M. Tignor, & H. L. Miller (Eds.), *Climate change 2007: The physical science basis. Contribution of working group I to the 4th assessment report of the Intergovernmental Panel on Climate Change*. Cambridge University Press.

Meinshausen, M., Smith, S. J., Calvin, K., Daniel, J. S., Kainuma, M. L. T., Lamarque, J. F., Matsumoto, K., Montzka, S. A., Raper, S. C. B., Riahi, K., Thomson, A., Velders, G. J. M., & van Vuuren, D. P. P. (2011). The RCP greenhouse gas concentrations and their extensions from 1765 to 2300. *Climatic Change*, *109*, 213–241. https://doi.org/10.1007/s10584-011-0156-z

Michelangeli, P. A., Vrac, M., & Loukos, H. (2009). Probabilistic downscalingapproaches: Application to wind cumulative distribution functions. *Geophysical Research Letters*, *36*, L11708. https://doi.org/10.1029/2009GL038401

Molina, M. O., Sánchez, E., & Gutiérrez, C. (2020). Future heat waves over the Mediterranean from an Euro-CORDEX regional climate model ensemble. *Scientific Reports*, *10*, 8801. https://doi.org/10.1038/s41598-020-65663-0

Molitor, D., Caffarra, A., Sinigoj, P., Pertot, I., Hoffmann, L., & Junk, J. (2014). Late frost damage risk for viticulture under future climate conditions: A case study for the Luxembourgish winegrowing region. *Australian Journal of Grape and Wine Research*, *20*, 160–168. https://doi.org/10.1111/ajgw.12059

Morales-Castilla, I., García de Cortázar-Atauri, I., Cook, B., Lacombe, T., Parker, A., van Leeuwen, C., Nicholas, K., & Wolkovich, E. (2020). Diversity buffers winegrowing regions from climate change losses. *Proceedings of the National Academy of Sciences of the United States of America*, *117*, 2864–2869. https://doi.org/10.1073/pnas.1906731117

Moriondo, M., Jones, G. V., Bois, B., Dibari, C., Ferrise, R., Trombi, G., & Bindi, M. (2013). Projected shifts of wine regions in response to climate change. *Climatic Change*, *119*(3–4), 825–839. https://doi.org/10.1007/s10584-013-0739-y

Mosedale, J. R., Wilson, R. J., & Maclean, I. M. D. (2015). Climate change and crop exposure to adverse weather: Changes to frost risk and grapevine flowering conditions. *PLoS ONE*, *10*(10), e0141218. https://doi.org/10.1371/journal.pone.0141218

Moss, R. H., Edmonds, J. A., Hibbard, K. A., Manning, M. R., Rose, S. K., van Vuuren, D. P., Carter, T. R., Emori, S., Kainuma, M., Kram, T., Meehl, G. A., Mitchell, J. F. B., Nakicenovic, N., Riahi, K., Smith, S. J., Stouffer, R. J., Thomson, A. M., Weyant, J. P., & Wilbanks, T. J. (2010). The next generation of scenarios for climate change research and assessment. *Nature*, *463*, 747–756. https://doi.org/10.1038/nature08823

Moutinho-Pereira, J. M., Correia, C. M., Goncalves, B. M., Bacelar, E. A., & Torres-Pereira, J. M. (2004). Leaf gas exchange and water relations of grapevines grown in three different conditions. *Photosynthetica*, *42*(1), 81–86. https://doi.org/10.1023/B:PHOT.0000040573.09614.1d

Nesbitt, A., Dorling, S., & Lovett, A. (2018). A suitability model for viticulture in England and Wales: Opportunities for investment, sector growth and increased climate resilience. *Journal of Land Use Science*, *13*, 414–438. https://doi.org/10.1080/1747423X.2018.1537312

Noble, A. C., Arnold, R. A., Masuda, B. M., Pecore, S. D., Schmidt, J. O., & Stern, P. M. (1984). Progress towards a standardized system of wine aroma terminology. *American Journal of Enology and Viticulture*, *35*(2), 107–109. https://www.ajevonline.org/content/35/2/107

OIV. (2019). *Statistical report on world vitiviniculture*. Author.

Parker, A. (2013). Modelling phenology and maturation of the grapevine Vitis Vinifera L.: Varietal differences and the role of leaf area to fruit weight ratio manipulations (Ph.D. thesis). Life Sciences. Lincoln University.

Parker, A., García de Cortázar-Atauri, I., Chuine, I., Barbeau, G., Bois, B., Boursiquot, J.-M., Cahurel, J.-Y., Claverie, M., Dufourcq, T., Gény, L., Guimberteau, G., Hofmann, R. W., Jacquet, O., Lacombe, T., Monamy, C., Ojeda, H., Panigai, L., Payan, J.-C., Lovelle, B. R., … van Leeuwen, C. (2013). Classification of varieties for their timing of flowering and veraison using a modelling approach: A case study for the grapevine species *Vitis vinifera* L. *Agricultural and Forest Meteorology*, *180*, 249–264. https://doi.org/10.1016/j.agrformet.2013.06.005

Parker, A. K., García de Cortázar-Atauri, I., Gény, L., Spring, J.-L., Destrac, A., Schultz, H., Molitor, D., Lacombe, T., Graça, A., Monamy, C., Stoll, M., Storchi, P., Trought, M., Hofmann, R., & van Leeuwen, C. (2020). Temperature-based grapevine sugar ripeness modelling for a wide range of *Vitis vinifera* L. cultivars. *Agricultural and Forest Meteorology*, *285–286*, 107902. https://doi.org/10.1016/j.agrformet.2020.107902

Poling, E. B. (2008). Spring cold injury to winegrapes and protection strategies and methods. *HortScience*, *43*, 1652–1662. https://doi.org/10.21273/HORTSCI.43.6.1652

Ramos, M. C., Jones, G. V., & Martinez-Casanovas, J. A. (2008). Structure and trends in climate parameters affecting winegrape production in northeast Spain. *Climate Research*, *38*, 1–15. https://doi.org/10.3354/cr00759

Riou, C., Becker, N., Sotes Ruiz, V., Gomez-Miguel, V., Carbonneau, A., Panagiotou, M., Calo, A., Costacurta, A., de Castro, R., Pinto, A., Lopes, C., Carneiro, L., & Climaco, P. (1994). *Le determinisme climatique de la maturation du raisin: Application au zonage de la teneur en sucre dans la Communauté Européenne*. Office des Publications Officielles des Communautés Européennes.

Robinson, J., Harding, J., & Vouillamoz, J. (2013). *Wine grapes: A complete guide to 1368 vine varieties, including their origins and flavours*. Penguin UK.

Samuelsson, P., Jones, C. G., Willen, U., Ullerstig, A., Gollvik, S., Hansson, U., Jansson, C., Kjellström, E., Nikulin, G., & Wyser, K. (2011). The Rossby Centre Regional Climate Model RCA3: Model description and performance. *Tellus A*, *63*(1), 4–23. https://doi.org/10.1111/j.1600-0870.2010.00478.x

Santos, J., Malheiro, A., Pinto, J., & Jones, G. (2012). Macroclimate and viticultural zoning in Europe: Observed trends and atmospheric forcing. *Climate Research*, *51*, 89–103. https://doi.org/10.3354/cr01056

Santos, J. A., Fraga, H., Malheiro, A. C., Moutinho-Pereira, J., Dinis, L. T., Correia, C., Moriondo, M., Leolini, L., Dibari, C., Costafreda-Aumedes, S., Kartschall, T., Menz, C., Molitor, D., Junk, J., Beyer, M., & Schultz, H. R. (2021). A review of the potential climate change impacts and adaptation options for European viticulture. *Applied Sciences*, *10*(9), 3092. https://doi.org/10.3390/app10093092

Schultz, H. R., & Jones, G. (2010). Climate induced historic and future changes in viticulture. *Journal of Wine Research*, *21*, 137–145. https://doi.org/10.1080/09571264.2010.530098

Sgubin, G., Swingedouw, D., Dayon, G., García de Cortázar-Atauri, I., Ollat, N., Page, C., & van Leeuwen, C. (2018). The risk of tardive frost damage in French vineyards in a changing climate. *Agricultural and Forest Meteorology*, *250–251*, 226–242. https://doi.org/10.1016/j.agrformet.2017.12.253

Sgubin, G., Swingedouw, D., Drijfhout, S., Mary, Y., & Bennabi, A. (2017). Abrupt cooling over the North Atlantic in modern climate models. *Nature Communications*, *8*. https://doi.org/10.1038/ncomms14375

Sgubin, G., Swingedouw, D., García de Cortázar-Atauri, I., Ollat, N., & van Leeuwen, C. (2019). The impact of possible decadal-scale cold-waves on viticulture over Europe in a context of global warming. *Agronomy*, *9*, 397. https://doi.org/10.3390/agronomy9070397

Sterl, A., Bintanja, R., Brodeau, L., Gleeson, E., Koenigk, T., Schmith, T., Semmler, T., Severijns, C., Wyser, K., & Yang, S. (2011). A look at the ocean in the EC-Earth climate model. *Climate Dynamics*, *39*, 2631–2657. https://doi.org/10.1007/s00382-011-1239-2

Swingedouw, D., Bily, A., Esquerdo, C., Borchert, L., Sgubin, G., Mignot, J., & Menary, M. (2021). On the risk of abrupt changes in the North Atlantic subpolar gyre in CMIP6 models. *Annals of the New York Academy of Sciences*, *1504*, 187–201. https://doi.org/10.1111/nyas.14659

Taylor, K. E., Stouffer, R., & Meehl, G. A. (2012). An overview of CMIP5 and the experiment design. *Bulletin of the American Meteorological Society*, *93*, 485–498. https://doi.org/10.1175/BAMS-D-11-00094.1

Tempere, S., Pérès, S., Espinoza, A. F., Darriet, P., Giraud-Héraud, E., & Pons, A. (2019). Consumer preferences for different red wine styles and repeated exposure effects. *Food Quality and Preference*, *73*, 110–116. https://doi.org/10.1016/j.foodqual.2018.12.009

Teslic, N., Vujadinović, M., Ruml, M., Ricci, A., Vukovic, A., Parpinello, G., & Versari, A. (2018). Future climatic suitability of the Emilia-Romagna (Italy) region for grape production. *Regional Environmental Change*, *19*, 599–614. https://doi.org/10.1007/s10113-018-1431-6

Teslic, N., Zinziani, G., Parpinello, G. P., & Versari, A. (2018). Climate change trends, grape production, and potential alcohol concentration in wine from the Romagna Sangiovese appellation area (Italy). *Theoretical and Applied Climatology*, *131*, 793–803. https://doi.org/10.1007/s00704-016-2005-5

Tomasi, D., Jones, G. V., Giust, M., Lovat, L., & Gaiotti, F. (2011). Grapevine phenology and climate change: Relationships and trends in the Veneto Region of Italy for 1964–2009. *American Journal of Enology and Viticulture*, *62*, 329–339. https://doi.org/10.5344/ajev.2011.10108

Tonietto, J., & Carbonneau, A. (2004). A multicriteria climatic classification system for grape-growing regions worldwide. *Agricultural and Forest Meteorology*, *124*, 81–97. https://doi.org/10.1016/j.agrformet.2003.06.001

Valdés-Gómez, H., Celette, F., García de Cortázar-Atauri, I., Jara-Rojas, F., Ortega-Farías, S., & Gary, C. (2009). Modelling soil water content and grapevine growth and development with the stics crop-soil model under two different water management strategies. *Journal International des Sciences de la Vigne et du Vin*, *43*(1), 13–28. https://doi.org/10.20870/oeno-one.2009.43.1.806

van Leeuwen, C., Barbe, J.-C., Darriet, P., Destrac-Irvine, A., Gowdy, M., Lytra, G., Marchal, A., Marchand, S., Plantevin, M., Poitou, X., Pons, A., & Thibon, C. (2022). Aromatic maturity is a cornerstone of terroir expression in red wine. *OENO One*, *56*(2), 335–351. https://doi.org/10.20870/oeno-one.2022.56.2.5441

van Leeuwen, C., & Darriet, P. (2016). The impact of climate change on viticulture and wine quality. *Journal of Wine Economics*, *11*(1), 150–167. https://doi.org/10.1017/jwe.2015.21

van Leeuwen, C., Destrac Irvine, A., Dubernet, M., Duchêne, E., Gowdy, M., Marguerit, E., Pieri, P., Parker, A., de Rességuier, L., & Ollat, N. (2019). An update on the impact of climate change in viticulture and potential adaptations. *Agronomy*, *9*. https://doi.org/10.3390/agronomy9090514

van Leeuwen, C., Garnier, C., Agut, C., Baculat, B., Barbeau, G., Besnard, E., Bois, B., Boursiquot, J.-M., Chuine, I., Dessup, T., Dufourcq, T., Garciacortazar, I., Marguerit, E., Monamy, C., Koundouras, S., Payan, J.-C., Parker, A., Renouf, V., Rodriguez-Lovelle, B., … Trambouze, W. (2008). Heat requirements for Grapevine varieties is essential information to adapt plant material in a Changing Climate. In: *Proceedings of the 7th International Terroir Congress*, Nyon, Switzerland, 19 May 2008; Vol. 1, pp. 222–227.

van Leeuwen, C., Schultz, H. R., García de Cortázar-Atauri, I., Duchêne, E., Ollat, N., Pieri, P., Bois, B., Goutouly, J.-P., Quénol, H., Touzard, J.-M., Malheiro, A. C., Bavaresco, L., & Delrot, S. (2013). Why climate change will not dramatically decrease viticultural suitability in main wine-producing areas by 2050. *Proceedings of the National Academy of Sciences of the United States of America*, *110*, E3051–E3052. https://doi.org/10.1073/pnas.1307927110

van Leeuwen, C., & Seguin, G. (2006). The concept of terroir in viticulture. *Journal of Wine Research*, *17*(1), 1–10. https://doi.org/10.1080/09571260600633135

van Leeuwen, C., Trégoat, O., Choné, X., Bois, B., Pernet, D., & Gaudillère, J. P. (2009). Vine water status is a key factor in grape ripening and vintage quality for red Bordeaux wine. How can it be assessed for vineyard management purposes? *Journal International des Sciences de la Vigne et du Vin*, *43*(3), 121–134. https://doi.org/10.20870/oeno-one.2009.43.3.798

Vautard, R., Noel, T., Li, L., Vrac, M., Martin, E., Dandin, P., & Joussaume, S. (2013). Climate variability and trends in downscaled high-resolution simulations and projections over metropolitan France. *Climate Dynamics*, *41*, 1419–1437. https://doi.org/10.1007/s00382-012-1621-8

Voldoire, A., Sanchez-Gomez, E., Salas y Mélia, D., Decharme, B., Cassou, C., Sénési, S., Valcke, S., Beau, I., Alias, A., Chevallier, M., Déqué, M., Deshayes, J., Douville, H., Fernandez, E., Madec, G., Maisonnave, E., Moine, M.-P., Planton, S., Saint-Martin, D., … Chauvin, F. (2013). The CNRM-CM5.1 global climate model: Description and basic evaluation. *Climate Dynamics*, *40*, 2091–2121. https://doi.org/10.1007/s00382-011-1259-y

Vrac, M., Drobinski, P., Merlo, A., Herrmann, M., Lavaysse, C., Li, L., & Somot, S. (2012). Dynamical and statistical downscaling of the French Mediterranean climate: Uncertainty assessment. *Natural Hazards and Earth System Sciences*, *12*, 2769–2784. https://doi.org/10.5194/nhess-12-2769-2012

Vrac, M., & Friederichs, P. (2015). Multivariate—intervariable, spatial, and temporal—Bias correction. *Journal of Climate*, *28*, 218–237. https://doi.org/10.1175/JCLI-D-14-00059.1

Vrac, M., Noel, T., & Vautard, R. (2016). Bias correction of precipitation through Singularity Stochastic Removal: Because occurrences matter. *Journal of Geophysical Research: Atmospheres*, *121*, 5237–5258. https://doi.org/10.1002/2015JD024511

Wang, E., & Engel, T. (1998). Simulation of phenological development of wheat crops. *Agricultural Systems*, *58*, 1–24. https://doi.org/10.1016/S0308-521X(98)00028-6

White, M. A., Diffenbaugh, N. S., Jones, G. V., Pal, J. S., & Giorgi, F. (2006). Extreme heat reduces and shifts United States premium wine production in the 21st century. *Proceedings of the National Academy of Sciences of the United States of America*, *103*(30), 11217–11222. https://doi.org/10.1073/pnas.0603230103

Yang, C., Menz, C., Fraga, H., Costafreda-Aumedes, S., Leolini, L., Ramos, M. C., Molitor, D., van Leeuwen, C., & Santos, J. A. (2022). Assessing the grapevine crop water stress indicator over the flowering-veraison phase and the potential yield lose rate in important European wine regions. *Agricultural Water Management*, *261*, 107349. https://doi.org/10.1016/j.agwat.2021.107349

SUPPORTING INFORMATION

Additional supporting information can be found online in the Supporting Information section at the end of this article.

How to cite this article: Sgubin, G., Swingedouw, D., Mignot, J., Gambetta, G. A., Bois, B., Loukos, H., Noël, T., Pieri, P., García de Cortázar-Atauri, I., Ollat, N., & van Leeuwen, C. (2023). Non-linear loss of suitable wine regions over Europe in response to increasing global warming. *Global Change Biology*, *29*, 808–826. https://doi.org/10.1111/gcb.16493